5.18 (t, J=5.4 Hz, 1H), 4.50 (dt, J=40.0 and 6.4 Hz, 2H), 4.37 (quint, J=3.5 Hz, 1H), 3.60 (m, 2H), 3.29 (m, 1H), 2.68 (td, J=6.2 and 3.3 Hz, 1H), 2.62 (td, J=6.0 and 3.7 Hz, 1H), 2.18 (d, J=4.0 Hz, 1H), 2.16 (d, J=3.8 Hz, 1H)
^{13}C NMR (DMSO-d_6, 75 MHz) δ 163.0, 150.6, 138.8, 109.1 (d, J=6.2 Hz), 82.8, 80.6, 73.4, 63.5, 60.2, 59.0, 41.2, 27.7 (d, J=21.2 Hz)
^{13}C NMR (100 MHz, $CDCl_3$) δ 163.0, 150.6, 138.8, 109.1 (d, J=6.2 Hz), 82.8, 80.6, 73.4, 63.5, 60.2, 59.0, 41.2, 27.7 (J=21.2 Hz)
UV λ_{max} (CH_3OH)=270 nm
m_p=196°C
FABMS, m/z=291 [M+H]
HRMS for $C_{11}H_{16}FN_2O_4S$: calculated=291.0815, found=291.0821.

The conditions of HPLC analysis are described in Section 2.15.

*2.6. N^3-(fluoromethyl)-thymidine (**1e**; NFT201)*

NFT201 was synthesized, using thymidine as a starting material, according to the procedure of Ogilvie et al. [32]. The purity of Compound **1e** was assessed by the conspicuous absence of impurities in the ^{1}H NMR spectrum and in HPLC (purity, 89.2%). The structure of the compound was based on its constitution (mass spectrometry), and the similarity of its ^{1}H NMR spectrum was based on other closely related molecules (thymidine and NFT202):

^{1}H NMR (CD_3OD, 500 MHz) δ 7.89 (s, 1H), 6.28 (t, J=6.5 Hz, 1H), 5.97 (d, J=50.5 Hz, 2H), 4.40 (quint, J=3.0 Hz, 1H), 3.92 (q, J=3.0 Hz, 1H), 3.80 (dd, J=12.5 and 3.0 Hz, 1H), 3.73 (dd, J=12.5 and 3.5 Hz, 1H), 2.28 (ddd, J=13.5, 6.5 and 3.5 Hz, 1H), 2.28 (ddd, J=13.5, 6.5 and 3.5 Hz, 1H), 2.22 (dd, J=13.5 and 3.5 Hz, 1H), 1.91 (s, 3H)
UV λ_{max} (CH_3OH)=271 nm
m_p=67–70°C
FABMS, m/z=275 [M+H]
HRMS for $C_{11}H_{16}FN_2O_5$: calculated=275.1044, found=275.0984.

The conditions of HPLC analysis are described in Section 2.15.

*2.7. N^3-(2-fluoroethyl)-thymidine (**1f**; NFT202)*

Using 2-fluoroethanol as a starting material, 2-fluoroethyltosylate was synthesized according to the method of Edgell and Parts [41]. 2-Fluoroethyltosylate (3.6 g, 17 mmol), potassium carbonate (4.6 g, 33 mmol) and thymidine (2.0 g, 8.3 mmol) were dissolved in an acetone:DMF (1:1) mixed solvent (500 ml), and the mixture was heated at 50°C for 7 h under argon atmosphere. The solvent was removed by rotary evaporation, and the desired product (**1f**; NFT202, 2.2 g, 94%) was purified by silica gel column chromatography (chloroform:methanol=5:1). The purity of Compound **1f** was assessed by the conspicuous absence of impurities in the ^{1}H NMR spectrum and in HPLC (purity, 98.4%):

^{1}H NMR (CD_3OD, 500 MHz) δ 7.85 (s, 1H, H-5), 6.29 (t, H-1′, $J_{1',2'a}$=$J_{1',2'b}$=5.6 Hz), 4.62, 4.53 (each t, each 1H, H-2″), 4.39 (m, 1H, H-3′), 4.25 (m, 2H, H-1″), 3.91(dd, 1H, H-5′ a, $J_{5'a,4'}$ =2.4, $J_{5'a,5'b}$=9.6 Hz), 3.80 (dd, 1H, H-5′ b, $J_{5'b,4'}$ =2.8, $J_{5'b,5'a}$=9.6 Hz), 3.72 (m, 1H, H-4′), 2.27 (ddd, 1H, H-2′ a, $J_{2'a,3'}$ =2.8, $J_{2'a,1'}$ =6.0, $J_{2'a,2'b}$=10.8 Hz), 2.21 (m, 1H, H-2′ b), 1.89 (s, 3H, 5-CH_3)
UV λ_{max} (CH_3OH)=267 nm
FABMS, m/z=289 [M+H]
HRMS for $C_{12}H_{18}FN_2O_5$: calculated =289.1200, found= 189.1230.

The conditions of HPLC analysis are described in Section 2.15.

*2.8. N^3-(3-fluoropropyl)-thymidine (**1g**; NFT203)*

1-Bromo-3-fluoropropane (5.0 g, 36 mmol), TBAF (16.2 g, 62 mmol) in THF (62 ml) and thymidine (1.5 g, 6.2 mmol) were dissolved in THF (40 ml), and the mixture was stirred at RT for 1 h under argon atmosphere. The solvent was removed by rotary evaporation, and the desired product (NFT203, 2.0 g, 100%) was purified by silica gel column chromatography (chloroform:methanol=5:1). The purity of Compound **1g** was assessed by the conspicuous absence of impurities in the ^{1}H NMR spectrum and in HPLC (purity, 97.8%):

^{1}H NMR (CD_3OD, 500 MHz) δ 7.82 (s, 1H, H-5), 6.28 (t, H-1′, $J_{1',2'a}$=$J_{1',2'b}$=5.6 Hz), 4.51, 4.42 (each t, each 1H, H-2″), 4.39 (m, 1H, H-3′), 4.04 (m, 2H, H-1″), 3.91 (dd, 1H, H-5′ a, $J_{5'a,4'}$ =2.4, $J_{5'a,5'b}$=9.6 Hz), 3.80 (dd, 1H, H-5′ b, $J_{5'b,4'}$ =2.8, $J_{5'b,5'a}$=9.6 Hz), 3.72 (m, 1H, H-4′), 2.27 (ddd, 1H, H-2′ a, $J_{2'a,3'}$ =2.8, $J_{2'a,1'}$ =6.0, $J_{2'a,2'b}$=10.8 Hz), 2.21 (m, 1H, H-2′ b), 1.95 (m, 1H, H-2″), 1.89 (s, 3H, 5-CH_3)
UV λ_{max} (CH_3OH)=268 nm
FABMS, m/z=303 [M+H]
HRMS for $C_{13}H_{20}FN_2O_5$: calculated=303.1356, found= 303.1372.

The conditions of HPLC analysis are described in Section 2.15.

*2.9. N^3-(2-fluoroethyl)-4′-thio-2′-deoxyuridine (**1h**; NFTS202)*

4′-Thio-thymidine was prepared from Compound **2**, according to the method of Otter et al. [34]. 2-Fluoro-1-bromoethane (127 mg, 1 mmol), cesium carbonate (195 mg, 0.6 mmol) and 4′ -thio-thymidine (129 mg, 0.5 mmol) were dissolved in DMF (5 ml), and the mixture was heated at 80°C for 10 h under argon atmosphere. The solvent was removed by rotary evaporation, and the desired product (NFTS202, 122 mg, 80%) was purified by silica gel column chromatography (chloroform:methanol=20:1). The purity

of Compound **1h** was assessed by the conspicuous absence of impurities in the ^{1}H NMR spectrum and in HPLC (purity, 92.7%):

^{1}H NMR (CD_3OD, 500 MHz) δ 6.60 (dd, H-1′, $J_{1',2'a}$=4.6, $J_{1',2'b}$=7.0 Hz), 5.74 (m, 1H, H-3′), 4.81 (dd, 1H, H-5′ a, $J_{5'a,4'}$ =2.4, $J_{5'a,5'b}$=10.0 Hz), 4.54–4.77 (m, 2H, H-5′ b, H-1″b), 4.60 (m, 1H, H-1″a), 4.55 (m, 1H, H-4′), 4.35 (m, 1H, H-2″a), 4.33 (m, 1H, H-2″a), 2.99 (ddd, 1H, H-2′ a, $J_{2'a,3'}$ =1.2, $J_{2'a,1'}$ =4.6, $J_{2'a,2'b}$=11.2 Hz), 2.83 (m, 1H, 2″-OH), 2.30 (ddd, 1H, H-2′ b, $J_{2'b,3'}$ =5.2, $J_{2'b,1'}$ =7.0, $J_{2'b,2'a}$=11.2 Hz), 1.65 (s, 3H, 5-CH_3)
UV λ_{max} (CH_3OH)=271 nm
FABMS, *m/z*=305 [M+H]
HRMS for $C_{12}H_{18}FN_2O_4S$: calculated=305.0971, found=305.1013.

The conditions of HPLC analysis are described in Section 2.15

*2.10. 1-(2-Deoxy-2-fluoro-β-D-arabinofuranosyl)-N^3-(2-fluoroethyl)-thymine (**1i**; NFAU202)*

FMAU was prepared by a four-step synthesis starting from 1,3,5-tri-*O*-benzoyl-α-D-ribofuranose, according to the procedure of Wilds and Damha [42]. 2-Fluoroethyltosylate (541 mg, 2.5 mmol), potassium carbonate (630 mg, 4.6 mmol) and FMAU (323 mg, 1.2 mmol) were dissolved in acetone:DMF (1:1; 30 ml), and the mixture was heated at 50°C for 8 h under argon atmosphere. The solvent was removed by rotary evaporation, and the desired product (NFAU202, 272 mg, 72%) was purified by silica gel column chromatography (chloroform:methanol=5:1). The purity of Compound **1i** was assessed by the conspicuous absence of impurities in the ^{1}H NMR spectrum and in HPLC (purity, 97.5%):

^{1}H NMR (CD_3OD, 500 MHz) δ 7.73 (s, 1H, H-5), 6.20 (dd, 1H, H-1′, $J_{1',F}$=17 Hz, $J_{1',2'}$ =4.0 Hz), 5.03 (dt, 1H, H-2′, $J_{2',F}$=52 Hz, $J_{1',2'}$ =$J_{2',3'}$ =2.5 Hz), 4.58 (dd, 2H, H-2″, $J_{2'',F}$=47 Hz, $J_{1',2'b}$=5.0 Hz), 4.32 (m, 1H, H-3′), 4.28 (m, 2H, H-1″), 3.91 (m, 1H, H-4′), 3.86 (dd, 1H, H-5′ a, $J_{5'a,4'}$ =12.0, $J_{5'a,5'b}$=4.0 Hz), 3.76 (dd, 1H, H-5′ b, $J_{5'b,4'}$ =12.0, $J_{5'b,5'a}$=4.0 Hz), 2.66 (s, 3H, 5-CH_3)
UV λ_{max} (CH_3OH)=265 nm
FABMS, *m/z*=307 [M+H]
HRMS for $C_{12}H_{17}F_2N_2O_5$: calculated=307.1106, found=307.1072.

The conditions of HPLC analysis are described in Section 2.15.

*2.11. 5-Fluoro-4′-thio-2′-deoxyuridine (**1l**; FTS901)*

The schematic diagram for the synthesis of Compound **1l** (FTS901) is depicted in Fig. 4. To an acetonitrile (8.7 ml) suspension of 5-fluorouracil (1.70 g, 13.0 mmol) was added BTMSA (5.66 g, 27.8 mmol), and the resultant mixture was stirred at RT for 2 h. The reaction mixture was added to MS4Å (ca. 4.3 g), an acetonitrile (8.7 ml) solution of Compound **2** (3.80 g, 8.70 mmol) and NIS (2.35 g, 10.4 mmol). The resultant mixture was stirred at RT for 22 h, filtered and concentrated in vacuo. The residue was dissolved with ethyl acetate, then the organic layer was washed with a 5% aqueous solution of sodium thiosulfate and a saturated aqueous solution of sodium hydrogen carbonate and brine. It was then dried with magnesium sulfate, filtered and concentrated in vacuo. The crude material was purified by silica gel column chromatography (eluent, hexane:ethyl acetate=3:2) to give 3′,5′-di-*O*-benzyl-5-fluoro-4′-thio-2′-deoxyuridine (**10**) (3.49 g, 91%, α:β=2:1):

β anomer ^{1}H NMR ($CDCl_3$, 300 MHz) δ 8.25 (d, *J*=6.6 Hz, 1H), 8.05 (br.s, 1H), 7.37–7.28 (m, 10H), 6.40 (t, *J*=6.6 Hz, 1H), 4.61–4.48 (m, 4H), 4.22 (q, *J*=3.7 Hz, 1H), 3.69 (q, *J*=3.7 Hz, 1H), 3.80–3.60 (m, 2H), 2.51 (ddd, *J*=13.6, 6.6 and 4.0 Hz, 1H), 2.15 (ddd, *J*=13.6, 7.7 and 4.4 Hz, 1H).

To a dichloromethane (3 ml) solution of Compound **10** (β anomer: 221 mg, 0.50 mmol) was added boron trichloride (1.0 M in dichloromethane solution, 2.0 ml, 2.0 mmol) at −78°C, and the resultant mixture was stirred at −78°C for 1 h. The mixture was quenched with a methanol

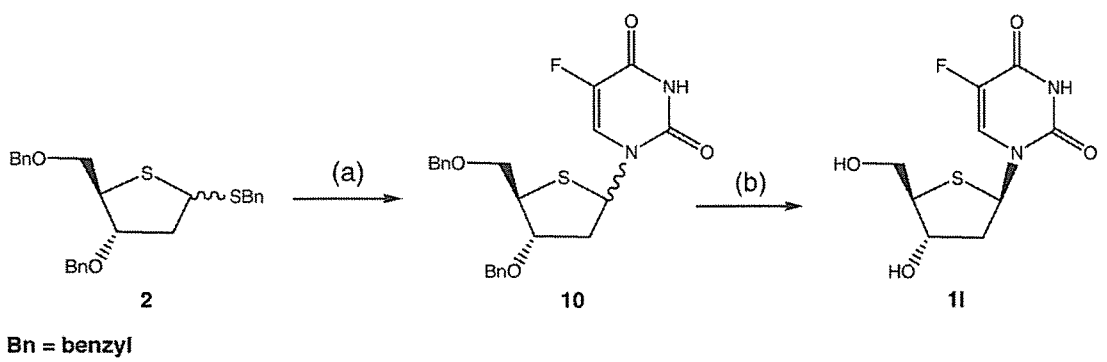

Fig. 4. Synthesis of Compound **1l** (FTS901). Conditions: (a) (i) 5-Fluorouracil, BTMSA, CH_3CN, RT; (ii) MS4Å, NIS, DMF, RT. (b) BCl_3, CH_2Cl_2, −78°C.

solution of ammonia (2.0 M, 3.0 ml), after which the mixture was warmed to RT and concentrated in vacuo. The residue was diluted with methanol and filtered, and the filtrate was concentrated in vacuo. The crude material was purified by silica gel column chromatography (eluent, chloroform:methanol=9:1) to give Compound **1l** (FTS901, 59 mg, 45%). The purity of Compound **1l** was assessed by the conspicuous absence of impurities in the ^{1}H NMR spectrum and in HPLC (purity, 97.6%):

^{1}H NMR (DMSO-d_6, 300 MHz) δ 11.84 (br.s, 1H), 8.33 (d, J=7.3 Hz, 1H), 6.23 (t, J=7.3 Hz, 1H), 5.24–5.19 (m, 1H), 4.35 (m, 1H), 3.65–3.55 (m, 2H), 3.31–3.28 (m, 1H), 2.25–2.15 (m, 2H)
^{13}C NMR (DMSO-d_6, 75 MHz) δ 157.5, 150.2, 142.1, 126.4, 74.4, 64.0, 61.8, 59.9, 42.2
UV λ_{max} (CH_3OH)=272 nm
FABMS, m/z=263 [M+H]
HRMS for $C_9H_{12}FN_2O_4S$: calculated=263.0502, found=263.0508.

The conditions of HPLC analysis are described in Section 2.15.

2.12. Expression and purification of recombinant human thymidine kinase

The preparation of recombinant human TK1 was carried out as described previously, with minor modifications [35]. The cDNA for human TK1 was amplified by polymerase chain reaction with plasmid pTK11 as template [43] and a pair of primers (5′-sense primer, 5′ CCATATGAGCTGCATTAACCTG; 3′-reverse complement primer, 5′ CGGGATCCCTCAGTTGGCAG) to create an *Nde*I site at the 5′-end and a *Bam*HI site at the 3′-end of the fragment. After treatment with *Nde*I and *Bam*HI, the TK1 fragment was ligated to plasmid pET-14b (EMD Biosciences Inc., San Diego, CA), which had been digested previously with the same restriction enzymes, to yield the expression plasmid pETMS207No.5. After being sequenced to confirm the correct insertion, pETMS207No.5 was transfected into *Escherichia coli* BL21 (DE3) pLys host cells. The expression of recombinant TK1 was induced with 0.4 mM isopropyl β-D-thiogalactopyranoside, and the protein was purified by affinity chromatography on chelated His·Bind resin (EMD Biosciences Inc.). The calculated molecular weight was 28 kDa for recombinant human TK1, and sodium dodecyl sulfate–polyacrylamide gel electrophoresis (SDS-PAGE) showed that the purity of TK1 was >95% (Fig. 5).

2.13. Phosphoryl transfer assay

Phosphoryl transfer assay with recombinant human TK1 was carried out as described previously, with minor modifications [35]. Briefly, nucleosides were dissolved in DMSO to make 100-mM stock solutions. The assays were carried out in reaction mixtures of 100 μM nucleosides (0.25% DMSO), 1 mM [γ-^{33}P]adenosine 5′-trisphosphate

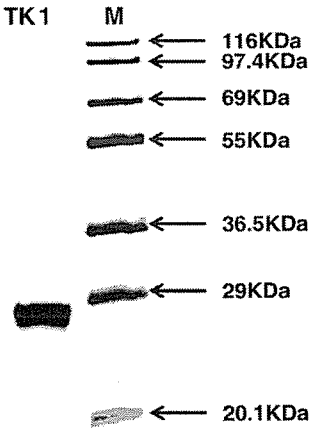

Fig. 5. SDS-PAGE of recombinant TK1 preparations. Two hundred nanograms of purified TK1 was loaded onto 12% gel. M, molecular weight markers.

(Amersham Biosciences, Piscataway, NJ), 50 mM Tris–HCl (pH 7.6), 5 mM $MgCl_2$, 15 mM NaF, 125 mM KCl, 10 mM dithiothreitol and 0.5% bovine serum albumin. The reaction was initiated by the addition of 60 ng of purified recombinant human TK1, and the reaction mixture was incubated for 15 min at 37°C. After being heated to 100°C for 3 min to stop the reaction, the mixture was centrifuged, and 2-μl samples were applied to PEI cellulose TLC plates (Merck Ltd., Darmstadt, Germany). The TLC plates were developed with isobutyric acid:ammonium hydroxide:water (66:1:33) for 12 h. The radioactivity on the plate was measured and quantified by a bioimaging analyzer (BAS-1500; Fuji Photo Film Co., Tokyo, Japan).

2.14. Transport assay

Transport assay was carried out as described previously, with minor modifications [44,45]. Briefly, 9-week-old male ddY mice were purchased from Japan SLC Inc. (Shizuoka, Japan) and were held for 1 week prior to the study. All procedures were performed in accordance with institutional guidelines (Guidelines for Animal Experiments, University of Fukui). The mice were asphyxiated with CO_2; blood was collected into a 3.8% citrate solution by cardiac puncture and used on the same day. After the removal of plasma and buffy coat, packed erythrocytes were washed with buffered saline (140 mM NaCl, 1.4 mM $MgSO_4$ and 18 mM Tris–HCl, at pH 7.4) and suspended in the same medium with a hematocrit of 11%. Nucleoside influx was initiated by the rapid addition of cell suspension to the buffered saline containing [2-^{14}C]thymidine (2.11 GBq/mmol; Amersham Biosciences) at four concentrations (0.05–0.5 mM) alone or together with various concentrations of test nucleosides. After 3 s, transport was terminated by the addition of 6-[(4-nitrobenzyl)thio]-9-β-D-ribofuranosylpurine (NBMPR; Sigma-Aldrich, St. Louis, MO) at a final concentration of 10 μM. Cells were pelleted

by an Eppendorf microcentrifuge (Model 5415D; Eppendorf Co., Ltd., Hamburg, Germany) at 12,800×*g* for 1 min and washed once with NBPMR solution. Cell pellets were extracted and chilled with 5% perchloric acid. After at least 30 min at 4°C, portions of the extracts were removed and counted in ACSII (Amersham Biosciences) by a liquid scintillation counter (LSC-5000; Aloka, Tokyo, Japan). The radioactivity trapped in the extracellular space of the pellet was measured in triplicate as a zero-time value by reversing the order in which NBMPR and nucleoside were added to the cells. This value was subtracted from the radioactivity of influx samples.

2.15. Degradation assay

To evaluate the stability of the N1–C′ 1 glycosidic bond, we tested the degradation of nucleosides by recombinant *E. coli* TP. Degradation assay was carried out as described previously, with minor modifications [46]. Briefly, the reaction mixture (final volume, 0.2 ml) contained 0.1 M potassium phosphate buffer (pH 7.4), 20 nmol of compounds and 0.015 U of recombinant *E. coli* TP (Sigma). The reaction was carried out at 25°C for 5, 15, 30 and 60 min, and terminated by adding 2 N perchloric acid (final concentration, 4%). After neutralization with potassium hydroxide, the resultant precipitate was removed by centrifugation. The supernatant was filtrated through a 4-mm Millex Syringe Filter Unit (Millipore, Bedford, MA), and a 10-μl aliquot was injected into the HPLC with a C18 (5-μm) analytical column [150×4.6 (i.d.) mm, Mightysil RP-18 GP Aqua; Kanto Chemical]. Elution was conducted by CH_3OH:H_2O:TFA [solvent compositions of CH_3OH:H_2O:TFA were as follows: 5:95:0.1 for FdUrd (**1k**); 10:90:0.1 for thymidine (**1a**); 15:85:0.1 for FT202 (**1b**), NFT201 (**1e**) and FTS901 (**1l**); 20:80:0.1 for FTS202 (**1d**), NFT203 (**1g**) and FLT (**1j**); 25:75:0.1 for NFT202 (**1f**) and NFAU202 (**1i**); and 30:70:0.1 for NFTS202 (**1h**)] at a flow rate of 0.8 ml/min and was monitored at 254 nm. Retention times were as follows: thymidine (**1a**), 8.4 min; FT202 (**1b**), 6.8 min; FTS202 (**1d**), 8.6 min; NFT201 (**1e**), 14.8 min; NFT202 (**1f**), 12.3 min; NFT203 (**1g**), 10.5 min; NFTS202 (**1h**), 8.4 min; NFAU202 (**1i**), 11.3 min; FLT (**1j**), 9.5 min; FdUrd (**1k**), 7.4 min; and FTS901 (**1l**), 7.0 min. Each compound was quantified by a comparison with the standard curve using the HPLC peak area of each standard compound.

3. Results

3.1. Phosphoryl transfer assay

The TK1 substrate characteristics of nucleosides were screened in phosphoryl transfer assays as a substrate for the recombinant human TK1 [47,48]. The data are summarized in Table 1. Among alkyl-fluorinated nucleosides, NFT202 (**1f**) had the highest value. The relative order of phosphorylation rates was as follows: thymidine (**1a**)>FdUrd (**1k**)>NFT202 (**1f**)=FLT (**1j**)>FTS101 (**1c**)>NFT201 (**1e**)=NFTS202 (**1h**)=FTS901 (**1l**)>FTS202 (**1d**)=NFT203 (**1g**)=FT202 (**1b**)>NFAU202 (**1i**). No correlation was observed between phosphorylation rates and fluoroalkyl length at the N3 position of thymidine. The 4′-thio substitution of FT202 did not reduce phosphorylation rates. In contrast, 4′ -thio substitution of NFT202 (**1f**) and FdUrd (**1k**) significantly reduced phosphorylation rates; the 2′-β-fluorine substitution of NFT202 (**1f**) further reduced such rates.

3.2. Transport assay

Transport assay was carried out as described previously, with minor modifications [44,45]. The concentration dependence of thymidine influx was portrayed on a Hanes–Woolf plot [49], yielding kinetic parameters of K_m=0.26±0.1 mM and V_{max}=17.54±6.82 pmol/μg packed erythrocytes/s. Competition among nucleosides with thymidine for entry at an external transporter site was demonstrated in influx competition experiments with [2-^{14}C]thymidine. The data were plotted according to Dixon [50]; examples are shown in Fig. 6A. For all compounds tested, the lines intersected at points above the [*I*] axis. Assuming that these data represent competitive inhibition [51], K_i values were determined by

Table 1
Phosphorylation of nucleosides by recombinant TK1, and K_i values of nucleosides in influx competition with thymidine

Compound	R_1	R_2	R_3	R_4	R_5	Phosphorylation (pmol/μg protein/h)	Relative phosphorylation	K_i (mM)
Thymidine (**1a**)	CH_3	H	O	H	OH	3008.05±749.40	1	0.26 (K_m)
FT202 (**1b**)	$F(CH_2)_2$	H	O	H	OH	697.03±87.20	0.23±0.03	0.53
FTS101 (**1c**)	FCH_2	H	S	H	OH	1117.08±87.28	0.37±0.03	0.55
FTS202 (**1d**)	$F(CH_2)_2$	H	S	H	OH	801.64±242.84	0.27±0.08	0.23
NFT201 (**1e**)	CH_3	FCH_2	O	H	OH	987.95±546.99	0.33±0.18	0.38
NFT202 (**1f**)	CH_3	$F(CH_2)_2$	O	H	OH	1424.32±218.82	0.47±0.07	0.53
NFT203 (**1g**)	CH_3	$F(CH_2)_3$	O	H	OH	486.49±198.59	0.26±0.06	0.51
NFTS202 (**1h**)	CH_3	$F(CH_2)_2$	S	H	OH	906.61±168.76	0.30±0.06	0.02
NFAU202 (**1i**)	CH_3	$F(CH_2)_2$	O	F	OH	17.42±0.71	0.01±0.00	0.51
FLT (**1j**)	CH_3	H	O	H	F	1431.89±100.59	0.48±0.03	2.69
FdUrd (**1k**)	F	H	O	H	OH	2571.06±151.38	0.85±0.05	0.70
FTS901 (**1l**)	F	H	S	H	OH	915.87±83.5	0.30±0.03	0.88

The results represent the mean±S.D. of at least three independent experiments.

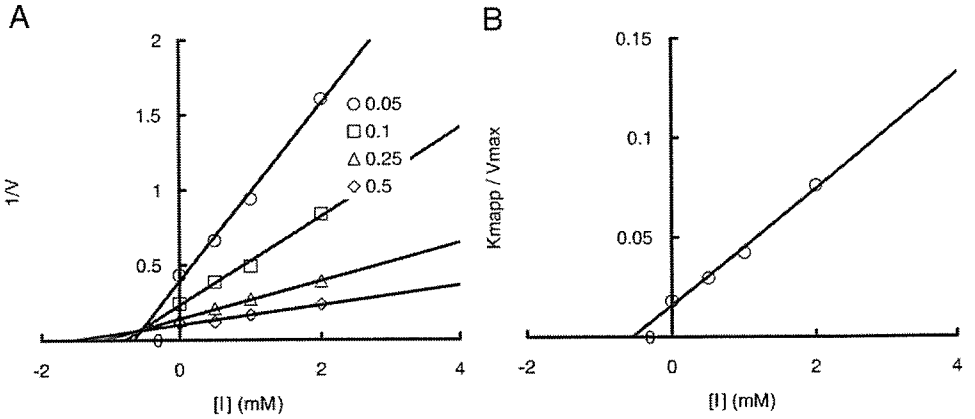

Fig. 6. An example of plots used for determining K_i values for nucleosides in influx competition experiments with thymidine. (A) An example of Dixon plots [50,51] of inhibition data. Each point represents the mean value of duplicate measurements from a single-cell suspension. Ordinates are expressed as picomoles of thymidine per microgram of packed erythrocytes per second, while those of the abscissa are FTS101 (**1c**) concentrations (in millimolars). Thymidine concentrations (mM) are shown in the legend. The lines were fitted by linear regression analysis. (B) K_{mapp} and V_{max} values were determined at each inhibitor concentration according to Eisenthal and Cornish-Bowden [52]. Shown is a replot of the ratios of these values as a function of FTS101 (**1c**) concentration [51]. [Units of the ordinate are expressed as: mM (pmol thymidine/μg packed erythrocytes/s)$^{-1}$.] The lines were fitted by linear regression analysis.

plotting influx competition data according to Eisenthal and Cornish-Bowden [52] to obtain K_{mapp} and V_{max} values and by replotting the ratio of these parameters as a function of [*I*] [51]; examples are shown in Fig. 6B. The K_i values are given in Table 1. These data showed that each of the eight nucleosides had an affinity for the transporter. FTS202 (**1d**) had affinities comparable to those of thymidine. The affinities of NFTS202 (**1h**) were 10 times those of thymidine. The other six alkyl-fluorinated nucleosides showed affinities that were 1.4–2.0 times lower than that of thymidine. FdUrd (**1k**) and FTS901 (**1l**) each showed affinities that were three times lower than that of thymidine. FLT (**1j**) showed affinities that were 10 times lower.

3.3. Degradation assay

Degradation assay was carried out as described previously, with minor modifications [46]. Table 2 shows the results. Except for FT202 (**1b**), there was no detectable glycosidic bond cleavage for 60 min in any of the alkyl-fluorinated nucleosides during incubations with recombinant *E. coli* TP. In contrast, under the same experimental conditions, thymidine (**1a**) underwent rapid glycosidic bond cleavage to give 57%, 89%, 98% and 99% thymidine (**1a**) degradation at 5, 15, 30 and 60 min, respectively. FdUrd (**1k**) and FTS901 (**1l**) also showed significant glycosidic bond cleavage to give 13%, 29%, 46% and 66% FdUrd (**1k**) degradation and 3%, 6%, 10% and 18% FTS901 (**1l**) degradation at 5, 15, 30 and 60 min, respectively. NFT202 (**1b**) underwent only slight time-dependent degradation to give 3%, 4% and 7% NFT202 (**1b**) degradation at 15, 30 and 60 min, respectively. As expected from previous findings, FLT (**1j**) did not show any significant glycosidic bond cleavage during the 60-min incubation with recombinant *E. coli* TP.

Table 2
Nucleosides as substrates for recombinant *E. coli* TP

Compound	R_1	R_2	R_3	R_4	R_5	Remaining nucleosides (%)				
						0 min	5 min	15 min	30 min	60 min
Thymidine (**1a**)	CH_3	H	O	H	OH	100.0±1.1	43.1±0.1	10.6±0.2	2.3±0.1	1.0±0.0
FT202 (**1b**)	$F(CH_2)_2$	H	O	H	OH	100.0±0.2	98.2±0.2	97.4±0.3	95.9±0.3	93.3±0.1
FTS101 (**1c**)	FCH_2	H	S	H	OH	ND	ND	ND	ND	ND
FTS202 (**1d**)	$F(CH_2)_2$	H	S	H	OH	100.0±0.2	99.4±0.3	99.1±0.3	99.3±0.2	98.9±0.1
NFT201 (**1e**)	CH_3	FCH_2	O	H	OH	100.0±2.4	100.9±1.7	98.7±1.7	101.7±0.3	102.0±0.9
NFT202 (**1f**)	CH_3	$F(CH_2)_2$	O	H	OH	100.0±0.5	98.8±1.2	98.7±1.0	99.6±0.9	99.0±0.5
NFT203 (**1g**)	CH_3	$F(CH_2)_3$	O	H	OH	100.0±0.7	99.7±0.6	99.5±0.4	98.0±0.1	99.4±0.2
NFTS202 (**1h**)	CH_3	$F(CH_2)_2$	S	H	OH	100.0±0.6	98.9±0.4	99.0±0.5	98.9±0.4	99.2±0.4
NFAU202 (**1i**)	CH_3	$F(CH_2)_2$	O	F	OH	100.0±0.1	99.4±0.2	99.2±0.4	99.2±0.4	99.1±0.2
FLT (**1j**)	CH_3	H	O	H	F	100.0±1.4	100.1±0.4	98.5±0.7	100.5±0.5	100.4±0.5
FdUrd (**1k**)	F	H	O	H	OH	100.0±0.3	87.1±0.3	71.2±0.4	54.4±0.1	34.1±0.9
FTS901 (**1l**)	F	H	S	H	OH	100.0±0.3	97.5±0.1	94.2±1.0	89.6±0.3	82.2±0.3

Values represent the mean±S.D. of at least three independent experiments of the remaining nucleoside as percentages of the total nucleoside in the reaction (100 μmol/L).
ND, not determined.

4. Discussion

In the last four decades, deoxynucleoside analogs have become increasingly important in the treatment of viral diseases and cancers. Nucleoside analogs are prodrugs requiring 5′-phosphorylation to form active nucleotides that can function as inhibitors of viral or cellular replication processes. Therefore, when labeled with a suitable radionuclide, some of these compounds have potential as radiopharmaceuticals for the noninvasive diagnosis of tumor cell proliferation. To be effective, they should: be selectively phosphorylated by TK1, be amenable to labeling with a positron-emitting or a single-photon-emitting radionuclide, have good in vivo stability and be transported across the cell membrane.

The present study examined those in vitro screens and finally selected NFT202 as a candidate for subsequent in vivo evaluation. This compound may be amenable to labeling with ^{18}F according to known methods.

All bioactive nucleosides have a β-configuration. In this study, Compounds **1b**, **1c**, **1d** and **1l** were obtained as α/β mixtures. The separation of α and β anomers of 3′,5′-di-*O*-*p*-toluoyl-5-(2-fluoroethyl)-2′-deoxyuridine was conducted by crystallization, as previously reported [30]. The melting point of Compound **1b** was also in agreement with the previously reported temperature (β anomer) [30].

The α and β anomers of Compounds **6**, **9** and **10** were easily separated by silica gel column chromatography. Compound **1l** was identified as a β anomer from the references [34]. The melting point of Compound **1d** was in agreement with the previously reported temperature of β anomer [27]. The β-isomer of Compound **1c** was rationally assigned by the result of a comparison of ^{1}H NMR with related β anomers (Compounds **1d** and **1l**).

The rationale of this study's drug design was based on the knowledge of 5-substituted 2′-deoxyuridines and carboranyl thymidine analogs. Many 5-substituted 2′-deoxyuridines, such as 5-fluoro-deoxyuridine, 5-chloro-deoxyuridine, 5-iodo-deoxyuridine, 5-bromo-deoxyuridine and 5-ethyl-2′-deoxyuridine, are good substrates for TK1 [47,48,53–56]. Analogs of 5-substituted 2′-deoxyuridines with bulky substitutions, such as 5-propenyl, 5-(2-chloroethyl)-2′-deoxyuridine and 5-(2-bromovinyl)-2′-deoxyuridine, are poor substrates for TK1 [53–55]. Therefore, we tried to evaluate the derivatives of 2′-deoxyuridine that contained a short-length fluoroalkyl chain at the C5 position, such as 5-(2-fluoroethyl), 5-(fluoromethyl)-4′-thio and 5-(2-fluoroethyl)-4′-thio derivatives of 2′-deoxyuridine. These 5-fluoroalkyl-substituted 2′-deoxyuridine derivatives were phosphorylated by human recombinant TK1. Among them, the compact 5-fluoromethyl substitution was the most effective substrate for TK1. However, the 5-fluoromethyl derivative is thought to be difficult to label with ^{18}F because attempts to synthesize the labeling precursor failed due to the labile nature of the leaving group. Thymidine analogs with methyl, ethyl and isopropyl, as well as various bulky *o*-carboranylalkyl substituents at the N3 position, were found to be surprisingly good substrates for TK1 [35,47,48,55–57]. These data indicate that TK1 can tolerate bulky groups at the N3 position of thymidine. In accordance with this hypothesis, TK1 effectively phosphorylated N^3-(fluoromethyl), N^3-(2-fluoroethyl), N^3-(3-fluoropropyl) and N^3-(2-fluoroethyl)-4′-thio derivatives of thymidine. Very recently, NFT202 was found to inhibit the phosphorylation of thymidine by recombinant TK1 [33]. Consistent with our results, NFT202 in that study retained its affinity for TK1 (IC_{50}=77–81 μg/ml). As expected by the poor phosphorylation activity of the parent fluorinated thymidine analog FMAU [21,22], its derivative (Compound **1i**) showed only minimal activity.

Nucleosides are hydrophilic and diffuse slowly across cell membranes. It is now well established that the permeation of nucleosides across the plasma membrane of mammalian cells is complex and is mediated by multiple transport proteins known as nucleoside transporters [58]. These transporters fall into two basic classes: (a) equilibrative (facilitated diffusion) carriers, which mediate both the influx and efflux of nucleosides, and (b) concentrative Na^+-dependent carriers, which, under physiological conditions, mediate only influx [58–61]. Based on sensitivity to 6-[(4-nitrobenzyl)thio]-9-β-D-ribofuranosylpurine (NBMPR), equilibrative transporters have been classified into two subtypes, equilibrative sensitive (*es*) and equilibrative insensitive (*ei*) [61–65]. The *es* subtype binds NBMPR with high affinity (K_d=1–10 nM) [66]. In contrast, the *ei* subtype is not affected by NBMPR at nanomolar concentrations and becomes inhibited only at high NBMPR concentrations (>10 μM) [66]. These two equilibrative transporters (*es* and *ei*) have been described in a large number of tumor cells and normal tissues. Especially, human tumor cell lines express predominantly NBMPR-sensitive transporters [67]. In contrast, concentrative transporters have been found predominantly in normal tissues, and only a limited number have been found in tumor cells [67]. Therefore, we focused on the transport assay with the NBMPR-sensitive mouse erythrocyte nucleoside transporter. However, inhibition constants, determined from our nucleoside transport assay, are assumed to reflect affinities for external binding sites on the transporter. Therefore, our results do not exactly provide evidence that the nucleoside transporter transports extracellular nucleosides into the cell. Additionally, in in vivo imaging, the expression and functional characteristics of nucleoside transporter families in the absorptive/excretory organs and target/nontarget cells will have important effects on the pharmacokinetics of tracers. Certainly, nucleoside transporters are crucial in determining the intracellular bioavailability and systemic disposition of nucleoside analogs. Knowledge of nucleoside transporters is important in the evaluation and prediction of the kinetics and targeting of nucleoside analogs. In this respect, our restricted transport screening system is

not helpful for predicting biodistribution. Therefore, our screening results cannot be applied directly beyond the in vitro situation.

Surprisingly, without any modification in the sugar moiety, thymidine that contains fluoroalkyl groups at the N3 position [N^3-(fluoromethyl)-thymidine, N^3-(2-fluoroethyl)-thymidine and N^3-(3-fluoropropyl)-thymidine] was not degraded during the 60-min incubations with recombinant *E. coli* TP. In contrast, thymidine was efficiently converted to thymine. Al-Madhoun et al. [47] reported that thymidine analogs containing the *o*-carboranylalkyl group at the 3-position were not substrates of recombinant TP. Our present finding also supports their results.

The development of a molecular imaging probe for positron emission tomography is based on a detailed understanding of cellular and molecular biochemistry. From this point of view, a recent report evaluating the kinetic uptake and retention of FLT in A549 cells should serve as a model for evaluating nucleoside analogs [25]. The DNA salvage pathway involves a futile cycle for nucleoside phosphorylation and dephosphorylation mediated by TK1 and a nucleotidase (dNT). This cycle poses an issue for interpreting tracer uptake values, since it provides a mechanism for the loss of established activity in cells. In proliferating cells, nucleoside analog metabolism takes place within the anabolic arm of the DNA salvage pathway. TK1 controls entry into the salvage pathway and converts intracellular nucleoside analogs to their nucleotide monophosphates [68]. Subsequent phosphorylations by other kinases within the DNA synthesis pathway [thymidylate kinase (TMPK) and nucleotide diphosphate kinase] lead to the added presence of nucleoside diphosphate and nucleoside triphosphate within cells. Intracellular thymidine labels DNA so rapidly that the impact of the retrograde synthesis of thymidine from thymidine triphosphate is negligible. Therefore, as was done for FLT, knowledge of the activities that dNT and TMPK have with regard to new nucleoside analogs would definitively show what analogs are appropriate for further study [25]. In fact, our companion work describes an in vitro and an in vivo evaluation of NFT202 (**1f**) showing that NFT202 (**1f**) was less effective than FLT (**1j**). Consequently, our limited selection criteria were not sufficient for discovering new nucleoside analogs for cell proliferation imaging.

In conclusion, derivatives of 2′-deoxyuridine that contain fluoroalkyl groups at the C5 position and derivatives of thymidine that contain fluoroalkyl groups at the N3 position were synthesized and examined in three in vitro assays designed to evaluate their potential as radiopharmaceuticals for imaging cellular proliferation. From these in vitro screening assays, we selected NFT202 as a candidate for subsequent in vivo evaluation because this compound met the three basic criteria of in vitro screening assays and also had the most potent phosphorylation activity as a substrate for recombinant human TK1. Additionally, this compound can be made amenable to labeling with ^{18}F according to known methods. Further investigation of the feasibility of ^{18}F-labeled NFT202 (**1f**) as a cell proliferation marker is described in separate papers.

Acknowledgments

We thank Mr. Kenji Frutuka for his excellent assistance with mass spectrometry analyses.

References

[1] Kubota R, Yamada S, Kubota K, Ishiwata K, Tamahashi N, Ido T. Intratumoral distribution of fluorine-18-fluorodeoxyglucose in vivo: high accumulation in macrophages and granulation tissues studied by microautoradiography. J Nucl Med 1992;33:1972–80.

[2] Yamada Y, Uchida Y, Tatsumi K, Yamaguchi T, Kimura H, Kitahara H, et al. Fluorine-18-fluorodeoxyglucose and carbon-11-methionine evaluation of lymphadenopathy in sarcoidosis. J Nucl Med 1998;39:1160–6.

[3] Strauss LG. Fluorine-18 deoxyglucose and false-positive results: a major problem in the diagnostics of oncological patients. Eur J Nucl Med 1996;23:1409–15.

[4] Shreve PD, Anzai Y, Whal RL. Pitfalls in oncologic diagnosis with FDG PET imaging: physiologic and benign variants. Radiographics 1999;19:61–77.

[5] Thorgeirsson SS, Okayama H. The United States–Japan cooperative cancer research program seminar on "Cell cycle control and cancer". Jpn J Cancer Res 1998;89:1093–7.

[6] Eary JF, Mankoff DA, Spence AM, Berger MS, Olshen A, Link JM, et al. 2-[C-11]Thymidine imaging of malignant brain tumors. Cancer Res 1999;59:615–21.

[7] Martiat P, Ferrant A, Labar D, Cogneau A, Boc C, Michel JL, et al. In vivo measurement of carbon-11 thymidine uptake in non-Hodgkin's lymphoma using positron emission tomography. J Nucl Med 1998;29:1633–7.

[8] Shields AF, Mankoff DA, Link JM, Graham MM, Eary JF, Kozawa SM, et al. Carbon-11-thymidine and FDG to measure therapy response. J Nucl Med 1998;39:1757–62.

[9] Vander Broght T, Pauwels S, Lambotte L, Labar D, De Maeght S, Stroobandt G, et al. Brain tumor imaging with PET and 2-[carbon-11]thymidine. J Nucl Med 1994;35:974–82.

[10] Van Eijkeren ME, De Schryver A, Goethals P, Poupeye E, Schelstraete K, Lemahieu I, et al. Measurement of short term ^{11}C-thymidine activity in human head and neck tumours using positron emission tomography (PET). Acta Oncol 1992;31:539–43.

[11] Blasberg RG, Roelcke U, Weinreich R, Beattie B, Ammon K, Yonekawa Y, et al. Imaging brain tumor proliferative activity with [^{124}I]iododeoxyuridine. Cancer Res 2000;60:624–35.

[12] Tjuvajev J, Muraki A, Ginos J, Berk J, Koutcher D, Ballon B, et al. Iododeoxyuridine (IUDR) uptake and retention as a measure of tumor growth. J Nucl Med 1993;34:1152–61.

[13] Tjuvajev JG, Macapinlac HA, Daghighian F, Scott AM, Ginos JZ, Finn RD, et al. Imaging of the brain tumor proliferative activity with [^{131}I]iododeoxyuridine. J Nucl Med 1994;35:1407–17.

[14] Wakanabe KA, Reichman U, Hirota K, Lopez C, Fox JJ. Nucleosides 110. Synthesis and antiherpes virus activity of some 2′-fluoro-2′-deoxyarabinofuranosylpyrimidine nucleosides. J Med Chem 1979;22:21–4.

[15] Alauddin MM, Conti PS, Fissekis JD. Synthesis of [^{18}F]-labeled 2′-deoxy-2′-fluoro-5-methyl-1-β-D-arabinofuranosyluracil ([^{18}F]-FMAU). J Label Compd Radiopharm 2002;45:583–90.

[16] Conti PS, Alauddin MM, Fissekis JR, Schmall B, Watanabe KA. Synthesis of 2′-fluoro-5-[^{11}C]-methyl-1-β-D-arabinofuranosyluracil

([^{11}C]-FMAU): a potential nucleoside analog for in vivo study of cellular proliferation with PET. Nucl Med Biol 1995;22:783–9.
[17] Mangner TJ, Klecker RW, Anderson L, Shields AF. Synthesis of 2′ -deoxy-2′ -[^{18}F]fluoro-β-D-arabinofuranosyl nucleosides, [^{18}F]FAU, [^{18}F]FMAU, [^{18}F]FBAU and [^{18}F]FIAU, as potential PET agents for imaging cellular proliferation. Synthesis of [^{18}F]labelled FAU. FMAU, FBAU, FIAU. Nucl Med Biol 2003;30:215–24.
[18] Sun H, Solan A, Mangner TJ, Vaishampayan U, Muzik O, Collins JM, et al. Imaging DNA synthesis with [^{18}F]FMAU and positron emission tomography in patients with cancer. Eur J Nucl Med Mol Imaging 2005;32:15–22.
[19] Grant AJ, Feinberg A, Chou TC, Watanabe KA, Fox JJ, Philips FS. Incorporation of metabolites of 2′ -fluoro-5-iodo-1-β-D-arabinofuranosylcytosine into deoxyribonucleic acid of neoplastic and normal mammalian tissues. Biochem Pharmacol 1982;31:1103–8.
[20] Shields AF, Grierson JR, Dohmen BM, Machulla HJ, Stayanoff JC, Lawhorn-Crews JM, et al. Imaging proliferation in vivo with [F-18]FLT and positron emission tomography. Nat Med 1998;4:1334–6.
[21] Cheng YC, Dutschman G, Fox JJ, Watanabe KA, Machida H. Differential activity of potential antiviral nucleoside analogs on herpes simplex virus-induced and human cellular thymidine kinases. Antimicrob Agents Chemother 1981;20:420–3.
[22] Wang J, Eriksson S. Phosphorylation of the anti-hepatitis B nucleoside analog 1-(2′ -deoxy-2′ -fluoro-1-β-D-arabinofuranosyl)-5-iodouracil (FIAU) by human cytosolic and mitochondrial thymidine kinase and implications for cytotoxicity. Antimicrob Agents Chemother 1996;40: 1555–7.
[23] Toyohara J, Waki A, Takamatsu S, Yonekura Y, Magata Y, Fujibayashi Y. Basis of FLT as a cell proliferation marker: comparative uptake studies with [^{3}H]thymidine and [^{3}H]arabinothymidine, and cell-analysis in 22 asynchronously growing tumor cell lines. Nucl Med Biol 2002;29:281–7.
[24] Grierson JR, Shields AF. Radiosynthesis of 3′ -deoxy-3′ -[^{18}F]fluorothymidine: [^{18}F]FLT for imaging of cellular proliferation in vivo. Nucl Med Biol 2000;27:143–56.
[25] Grierson JR, Schwartz JL, Muzi M, Jordan R, Krohn KA. Metabolism of 3′ -deoxy-3′ -[F-18]fluorothymidine in proliferating A549 cells: validations for positron emission tomography. Nucl Med Biol 2004;31:829–37.
[26] Ditmann H, Dohman BM, Kehlbach R, Bartusek G, Pritzkow M, Sarbia M, et al. Early changes in [^{18}F]FLT uptake after chemotherapy: an experimental study. Eur J Nucl Med Mol Imaging 2002;29:1462–9.
[27] Rahim SG, Trivedi N, Bogunovic-Batchelor MV, Hardy GW, Mills G, Selway JW, et al. Synthesis and anti-herpes virus activity of 2′ -deoxy-4′ -thiopyrimidine nucleosides. J Med Chem 1996;39:789–95.
[28] Toyohara J, Hayashi A, Sato M, Tanaka H, Haraguchi K, Yoshimura Y, et al. Rationale of 5-^{125}I-4′ -thio-2′ -deoxyuridine as a potential iodinated proliferation marker. J Nucl Med 2002;43:1218–26.
[29] Toyohara J, Gogami A, Hayashi A, Yonekura Y, Fujibayashi Y. Pharmacokinetics and metabolism of 5-^{125}I-4′ -thio-2′ -deoxyuridine in rodents. J Nucl Med 2003;44:1671–6.
[30] Griengl H, Wanek E, Schwarz W, Steicher W, Rosenwirth B, Clercq ED. 2′ -Fluorinated arabinonucleosides of 5-(2-haloalkyl)uracil: synthesis and antiviral activity. J Med Chem 1987;30:1199–204.
[31] Walker R, Coe P, Rahim SG. Further antiviral pyrimidine nucleosides. International Publication WO9104982.
[32] Ogilvie KK, Beaucage SL, Gillen MF, Entwistle D, Quilliam M. Fluoride ion catalyzed alkylation of purines, pyrimidines, nucleosides and nucleotides using alkyl halides. Nucleic Acid Res 1979;6: 1695–708.
[33] Balzarini J, Celen S, Karlsson A, de Groot T, Verbruggen A, Bormans G. The effect of a methyl or 2-fluoroethyl substituent at the N-3 position of thymidine, 3′ -fluoro-3′ -deoxythymidine and 1-β-D-arabinosylthymine on their antiviral and cytostatic activity in cell culture. Antivir Chem Chemother 2006;17:17–23.
[34] Otter GP, Elzagheid MI, Johens GD, MacCulloch AC, Walker RT, Oivanen M, et al. Synthesis and hydrolytic stability of the α and β anomers of 4′ -thio-2′ -deoxyuridine and their 5-substituted analogs. Competition between the acid-catalysed depyrimidination and isomerisation to 5-thiopyranoside nucleoside. J Chem Soc Perkin Trans 1998;2:2343–9.
[35] Lunato AJ, Wang J, Woollard JE, Anisuzzaman AKM, Ji W, Rong FG, et al. Synthesis of 5-(carboranylalkylmercapto)-2′ -deoxyuridines and 3-(carboranylalkyl)thymidines and their evaluation as substrates for human thymidine kinases 1 and 2. J Med Chem 1999;42:3378–89.
[36] Chi DY, Kilbour MR, Katzenellenbogen JA, Brodack JW, Welch MJ. Synthesis of no-carrier-added *N*-([^{18}F]fluoroalkyl)spiperone derivatives. Appl Radiat Isot 1986;37:1173–80.
[37] Sasaki T, Minamoto K, Suzuki H. Elimination reaction on the di- and trimesylated derivatives of N^3-benzyluridine. J Org Chem 1973;38: 598–607.
[38] Yamamoto I, Kimura T, Tateoka Y, Watanabe K, Ho IK. *N*-substituted oxopyrimidines and nucleosides: structure–activity relationship for hypnotic activity as central nervous system depressant. J Med Chem 1987;30:2227–31.
[39] Fissekis JD, Myles A, Brown GB. Synthesis of 5-hydroxyalkylpyrimidines from lactones. J Org Chem 1964;29:2670–3.
[40] Dyson MR, Coe PL, Walker RT. An improved synthesis of benzyl 3,5-di-*O*-benzyl-2-deoxy-1,4-dithio-D-*erythro*-pentofuranoside, an intermediate in the synthesis of 4′ -thionucleosides. Carbohydr Res 1991;216:237–48.
[41] Edgell WF, Parts L. Synthesis of alkyl and substituted alkyl fluorides from *p*-toluenesulfonic acid esters. The preparation of *p*-toluenesulfonic acid esters of lower alcohols. J Am Chem Soc 1955;77:4899–902.
[42] Wilds CJ, Damha MJ. 2′ -Deoxy-2′ -fluoro-β-D-arabinonucleosides and oligonucleotides (2′ F-ANA): synthesis and physicochemical studies. Nucleic Acids Res 2000;28:3625–35.
[43] Bradshaw Jr MD, Deininger PL. Human thymidine kinase gene: molecular cloning and nucleotide sequence of a cDNA expressible in mammalian cells. Mol Cell Biol 1984;11:2316–20.
[44] Gati P, Misra HK, Knaus EE, Wiebe LI. Structural modifications at the 2′ - and 3′ -positions of some pyrimidine nucleosides as determinations of their interaction with the mouse erythrocyte nucleoside transporter. Biochem Pharmacol 1984;33:3325–31.
[45] Gati WP, Knaus EE, Wiebe LI. Interaction of 2′ -halogeno-2′ -deoxyuridines with the human erythrocyte nucleoside transport mechanism. Mol Pharmacol 1983;23:146–52.
[46] Komatsu T, Yamazaki H, Shimada N, Nagayama S, Kawaguchi Y, Nakajima M, et al. Involvement of microsomal cytochrome p450 and cytosolic thymidine phosphorylase in 5-fluorouracil formation from tegaful in human liver. Cancer Res 2001;7:675–81.
[47] Al-Madhoun AS, Johnsamuel J, Barth RF, Tjarks W, Eriksson S. Evaluation of human thymidine kinase 1 substrates as new candidates for boron neutron capture therapy. Cancer Res 2004;64: 6280–6.
[48] Byun Y, Yan J, Al-Madhoun AS, Johnsamuel J, Yang W, Barth RF, et al. Synthesis and biological evaluation of neutral and zwitterionic 3-carboranyl thymidine analogues for boron neutron capture therapy. J Med Chem 2005;48:1188–98.
[49] Hanes CS. Studies of plant amylases: I. The effect of starch concentration upon the velocity of hydrolysis by the amylase of germinated barley. Biochem J 1932;26:1406–21.
[50] Dixon M. The determination of enzyme inhibitor constants. Biochem J 1953;55:170–1.
[51] Dixon M, Webb EC. Inhibitors. In: Dixon EC, Webb DC, editors. Enzymes. 3rd ed. London: Longman; 1979. p. 332–80.
[52] Eisenthal R, Cornish-Bowden A. The direct linear plot. A new graphical procedure for estimating enzyme kinetic parameters. Biochem J 1974;139:715–20.
[53] Johansson NG, Eriksson S. Structure–activity relationships for phosphorylation of nucleoside analogs to monophosphates by nucleoside kinases. Acta Biochim Pol 1996;43:143–60.

[54] Eriksson S, Kierdaszuk B, Munch-Petersen B, Öberg B, Johansson NG. Comparison of the substrate specificities of human thymidine kinase 1 and 2 and deoxycytidine kinase toward antiviral and cytostatic nucleoside analogs. Biochem Biophys Res Commun 1991;176:586–92.

[55] Al-Madhoun AS, Tjarks W, Eriksson S. The role of thymidine kinases in the activation of pyrimidine nucleoside analogs. Mini Rev Med Chem 2004;4:341–50.

[56] Al-Madhoun AS, Johansamuel J, Yan J, Ji W, Wang J, Zhou JC, et al. Synthesis of a small library of 3-(carboranylalkyl)thymidines and their biological evaluation as substrates for human thymidine kinase 1 and 2. J Med Chem 2002;45:4018–28.

[57] Tjarks W, Wang J, Chandra S, Ji W, Zhuo J, Lunato AJ, et al. Synthesis and biological evaluation of boronated nucleosides for boron neutron capture therapy (BNCT) of cancer. Nucleosides Nucleotides Nucleic Acids 2001;20:695–8.

[58] Kong W, Engel K, Wang J. Mammalian nucleoside transporters. Curr Drug Metab 2004;5:63–84.

[59] Paterson ARP, Cass CE. Transport of nucleoside drugs in animal cells. In: Goldman ID, editor. Membrane transport of antineoplastic agents. New York: Pergamon Press; 1986. p. 309–29.

[60] Plagemann PGW, Wohlhueter RM. Permeation of nucleosides, nucleic acid bases, and nucleotides in animal cells. Curr Top Membr Transp 1980;14:225–330.

[61] Jarvi SM. Adenosine transporters. In: Cooper DMF, Londons C, editors. Adenosine receptors. New York: Alan R. Liss, Inc.; 1988. p. 113–23.

[62] Belt JA. Heterogeneity of nucleoside transport in mammalian cells. Two types of transport activity in L1210 and other cultured neoplastic cells. Mol Pharmacol 1983;24:479–84.

[63] Plagemann PGW, Wohlhueter RM. Nucleoside transport in cultured mammalian cells. Multiple forms with different sensitivity to inhibition by nitrobenzylthioinosine or hypoxantine. Biochem Biophys Acta 1984;773:39–52.

[64] Belt JA, Noel LD. Nucleoside transport in walker 256 rat carcinosarcoma and S49 mouse lymphoma cells. Biochem J 1985; 232:681–8.

[65] Jarvis SM, Young JD. Nucleoside transport in rat erythrocytes: two components with differences in sensitivity to inhibition by nitrobenzylthioinosine and *p*-chloromercuryphenyl sulfonate. J Membr Biol 1986;93:1–10.

[66] Griffith DA, Jarvis SM. Nucleoside and nucleobase transport systems of mammalian cells. Biochem Biophys Acta 1996;1286:153–81.

[67] Belt JA, Marina NM, Phelps DA, Crawford CR. Nucleoside transport in normal and neoplastic cells. Adv Enzyme Regul 1993;33:235–52.

[68] Kornberg A, Baker TA. Biosynthesis of DNA precursors. In: Kornberg A, Baker TA, editors. DNA replication. 2nd ed. New York: Freeman; 1992. p. 53–100.

資料(3)

資料 3

Available online at www.sciencedirect.com

ScienceDirect

Nuclear Medicine and Biology 33 (2006) 765–772

NUCLEAR MEDICINE — AND — BIOLOGY

www.elsevier.com/locate/nucmedbio

Alkyl-fluorinated thymidine derivatives for imaging cell proliferation II. Synthesis and evaluation of N^3-(2-[^{18}F]fluoroethyl)-thymidine

Jun Toyohara[a,*], Akio Hayashi[b], Akie Gogami[b], Yasuhisa Fujibayashi[c]

[a]*Probe Research Section, Department of Molecular Probe, Molecular Imaging Center, National Institute of Radiological Sciences, Chiba 263-8555, Japan*
[b]*Research and Development Division, Research Center, Nihon Medi-Physics Co., Ltd., Chiba, Japan*
[c]*Biomedical Imaging Research Center, University of Fukui, Fukui, Japan*

Received 17 January 2006; revised 16 May 2006; accepted 11 June 2006

Abstract

We prepared N^3-(2-[^{18}F]fluoroethyl)-thymidine ([^{18}F]NFT202) and examined its potential as a positron emission tomography (PET) ligand for imaging cellular proliferation. [^{18}F]NFT202 was synthesized from 3′,5′-di-*O*-toluoyl-N^3-(2-*p*-toluenesulfoxyethyl)-thymidine in a two-step reaction. N^3-(2-fluoroethyl)-[2-^{14}C]thymidine ([^{14}C]NFT202) was also synthesized from [2-^{14}C]thymidine in a one-step reaction. Whereas [^{18}F]NFT202 did not accumulate in mouse Lewis lung carcinoma tumors, 3′-[^{18}F]3′-fluoro-3′-deoxythymidine ([^{18}F]FLT) showed significantly high uptake. To clarify this unexpected result, we evaluated the cell uptake of [^{14}C]NFT202 in vitro. The uptake was approximately eight times higher in thymidine kinase 1 (TK1)$^+$ clones (L-M cells) than in TK1-deficient mutant L-M(TK$^-$) cells ($P<.01$, Student's t test). In addition, we observed a positive correlation between tracer uptake and the S-phase fraction. However, the net in vitro tumor cell uptake of [^{14}C]NFT202 was lower than that of [2-^{14}C]3′-fluoro-3′-deoxythymidine. [^{14}C]NFT202 was not effectively incorporated into the DNA fraction and was indeed washed out from tumor cells. These results clearly showed that [^{18}F]NFT202 did not surpass the performance of [^{18}F]FLT. We therefore conclude that [^{18}F]NFT202 is not a suitable PET ligand for imaging tumor cell proliferation.

Keywords: Nucleosides; Positron emission tomography; Proliferation; [^{18}F]NFT202

1. Introduction

During the last four decades, deoxynucleoside analogs have grown increasingly important in the treatment of viral diseases and cancers. Nucleoside analogs are prodrugs requiring 5′-phosphorylation to form active nucleotides that can function as inhibitors of viral or cellular replication processes. Therefore, when labeled with a suitable radionuclide, some of these compounds have potential use as radiopharmaceuticals for the noninvasive diagnosis of tumor cell proliferation. To be effective in that role, these compounds should have at least the following attributes: (a) they should be selectively phosphorylated by thymidine kinase 1 (TK1); (b) they should be labeled with a positron-emitting or a single-photon-emitting radionuclide; (c) they should exhibit good in vivo stability; and (d) their transport across cell membranes should be rapid.

In a separate paper, our group identified the N^3 fluoroethylated derivative of thymidine, N^3-(2-fluoroethyl)-thymidine (subsequently referred to as NFT202), as a potential agent of cellular proliferation imaging by virtue of three basic properties: (a) it is resistant to glycosidic bond cleavage; (b) its phosphorylation by TK1 is comparable to that by thymidine; and (c) it has an affinity for mammalian 6-[(4-nitroxyl)thiol]-9-β-D-ribofuranosylpurine-sensitive nucleoside transporters. Therefore, we expected fluorine-18-labeled NFT202 to be a suitable tracer for cellular proliferation imaging by positron emission tomography (PET).

In this paper, we describe the synthesis of N^3-(2-[^{18}F]fluoroethyl)-thymidine ([^{18}F]NFT202; **6**) and examine its potential as a PET ligand for imaging cellular proliferation. Despite its acceptable properties in vitro, [^{18}F]NFT202 did not accumulate in tumors. To clarify this result and the uptake mechanism of [^{18}F]NFT202, we also performed an in vitro cell uptake study with N^3-(2-fluoroethyl)-[2-^{14}C]thymidine ([^{14}C]NFT202). Based on resultant data, we concluded that [^{18}F]NFT202 is not a suitable PET ligand for imaging tumor cell proliferation.

* Corresponding author. Tel.: +81 43 206 4041; fax: +81 43 206 3261.
E-mail address: toyohara@nirs.go.jp (J. Toyohara).

0969-8051/$ – see front matter © 2006 Elsevier Inc. All rights reserved.
doi:10.1016/j.nucmedbio.2006.06.001

Moreover, in a number of important ways, this paper parallels previous validation studies with FLT, particularly uptake/washout studies in A549 cells [1]. Nucleoside tracer validation is also discussed.

2. Materials and methods

2.1. Radiochemicals

[2-^{14}C]3′-Fluoro-3′-deoxythymidine ([^{14}C]FLT; 1.961 GBq/mmol, 3.7 MBq/ml) was purchased from Moravek Biochemicals, Inc. (Brea, CA, USA). [2-^{14}C]Thymidine ([^{14}C]Thd; 2.18 GBq/mmol, 3.7 MBq/ml) was purchased from Amersham Biosciences (Piscataway, NJ, USA).

2.2. 3′,5′-Di-O-toluoyl thymidine (2)

p-Toluoyl chloride (2.1 ml, 16.1 mmol) was added to a solution of thymidine (**1**) (1.95 g, 8 mmol) in pyridine (80 ml) under argon atmosphere. The mixture was stirred for 16 h at room temperature and then poured into ice water. After being stirred for 5 min, the precipitated product was collected, washed with water and dried. The desired product (**2**; 3.4 g, 7.1 mmol, 89%) was purified by silica gel column chromatography (*n*-hexane:ethyl acetate=3:1):

^{1}H nuclear magnetic resonance (NMR) (CD_3OD, 500 MHz): δ 8.45 (bs, 1H, NH), 7.69 (m, 4H, *o*-Tol), 7.26 (m, 5H, H-6, *m*-Tol), 6.46 (dd, H-1′, $J_{1',\ 2'a}$=4.4 Hz, $J_{1',\ 2'b}$=6.8 Hz), 5.64 (m, 1H, H-3′), 4.79 (dd, 1H, H-5′a, $J_{5'a,\ 4'}$=2.8 Hz, $J_{5'a,\ 5'b}$=9.6 Hz), 4.65 (dd, 1H, H-5′b, $J_{5'b,\ 4}$=2.8 Hz, $J_{5'b,\ 5'a}$=9.6 Hz), 5.53 (m, 1H, H-4′), 2.70 (ddd, 1H, H-2′a, $J_{2'a,\ 3'}$=1.2 Hz, $J_{2'a,\ 1'}$=4.4 Hz, $J_{2'a,\ 2'b}$=11.2 Hz), 2.44, 2.43 (each s, each 3H, Tol-CH_3), 2.31 (ddd, 1H, H-2′b, $J_{2'b,\ 3'}$=5.2 Hz, $J_{2'b,\ 1'}$=6.8 Hz, $J_{2'b,\ 2'a}$=11.2 Hz), 1.62 (s, 3H, 5-CH_3)

^{13}C NMR ($CDCl_3$, 100 MHz): δ 166.10, 166.04, 163.06, 150.11, 144.64, 134.44, 129.85, 129.53, 129.51, 129.32, 126.54, 126.25, 111.64, 84.91, 82.82, 77.28, 74.91, 64.18, 38.08, 21.76, 21.72, 12.13

mp=200°C

Fast atom bombardment mass spectrometry (FAB-MS): *m/z*=479 [M+H]

High-resolution mass spectrometry (HRMS) for $C_{26}H_{27}N_2O_7$: calculated=479.1819, found=479.1755.

2.3. 3′,5′-Di-O-toluoyl-N^3-(2-hydroxyethyl)-thymidine (3)

Tetrabutylammonium fluoride (TBAF; 20.9 g, 80 mmol) in tetrahydrofuran (THF; 80 ml) and 2-bromoethanol (14 ml, 0.2 mmol) was added to a solution of Compound **2** (3.7 g, 8 mmol) in THF (120 ml) under argon atmosphere. The mixture was stirred for 2 h at room temperature and then poured into ice water. After having been stirred for 5 min, the precipitated product was collected, washed with water and dried (**3**; 3.3 g, 6.5 mmol, 81%):

^{1}H NMR (CD_3OD, 500 MHz): δ 7.96 (m, 4H, *o*-Tol), 7.26 (m, 5H, H-6, *m*-Tol), 6.48 (dd, H-1′, $J_{1',\ 2'a}$=4.4 Hz, $J_{1',\ 2'b}$=6.8 Hz), 5.64 (m, 1H, H-3′), 4.79 (dd, 1H, H-5′a, $J_{5'a,\ 4'}$=2.8 Hz, $J_{5'a,\ 5'b}$=9.6 Hz), 4.66 (dd, 1H, H-5′b, $J_{5'b,\ 4}$=2.8 Hz, $J_{5'b,\ 5'a}$=9.6 Hz), 5.53 (m, 1H, H-4′), 4.21 (m, 1H, H-1′), 3.86 (m, 1H, H-2′), 2.72 (ddd, 1H, H-2′a, $J_{2'a,\ 3'}$=1.2 Hz, $J_{2'a,\ 1'}$=4.4 Hz, $J_{2'a,\ 2'b}$=11.2 Hz), 2.53 (m, 1H, 2′-OH), 2.44, 2.43 (each s, each 3H, Tol-CH_3), 2.31 (ddd, 1H, H-2′b, $J_{2b,\ 3'}$=5.2 Hz, $J_{2b,\ 1'}$=6.8 Hz, $J_{2b,\ 2'a}$=11.2 Hz), 1.65 (s, 3H, 5-CH_3)

^{13}C NMR ($CDCl_3$, 100 MHz) δ 166.06, 166.34, 164.12, 151.56, 144.61, 132.93, 129.81, 129.51, 129.48, 129.30, 126.51, 126.25, 110.99, 85.75, 82.85, 77.25, 74.89, 64.13, 61.79, 43.97, 38.19, 21.73, 21.69, 12.84

mp=180°C

FAB-MS: *m/z*=523 [M+H]

HRMS for $C_{28}H_{31}N_2O_8$: calculated=523.2081, found=523.2026.

2.4. 3′,5′-Di-O-toluoyl-N^3-(2-p-toluenesulfoxyethyl)-thymidine (4)

p-Toluenesulfonyl chloride (229 mg, 1.2 mmol) was added to a solution of Compound **3** (552 mg, 1.0 mmol) in pyridine (10 ml) under argon atmosphere. The mixture was stirred for 16 h at 0°C. After dilution with 50 ml of chloroform, the organic layer was washed with 1 N hydrochloric acid (40 ml), water (40 ml), saturated sodium hydrogen carbonate solution (40 ml) and saturated sodium chloride solution (40 ml). It was then dried by anhydrous sodium sulfate and concentrated. The solvent was removed by rotary evaporation, and the desired product (**4**; 550 mg, 0.74 mmol, 74%) was purified by silica gel column chromatography (n-hexane:ethyl acetate=1:1):

^{1}H NMR (CD_3OD, 500 MHz): δ 7.96 (m, 4H, *o*-Tol), 7.69 (m, 2H, *o*-Ts), 7.26 (m, 7H, H-6, *m*-Tol, *m*-Ts), 6.44 (dd, H-1′, $J_{1',\ 2'a}$=4.4 Hz, $J_{1',\ 2'b}$=6.8 Hz), 5.63 (m, 1H, H-3′), 4.81 (dd, 1H, H-5′a, $J_{5'a,\ 4'}$=2.4 Hz, $J_{5'a,\ 5'b}$=10.0 Hz), 4.65 (dd, 1H, H-5′b, $J_{5'b,\ 4}$=2.8 Hz, $J_{5'b,\ 5'a}$=10.0 Hz), 5.54 (m, 1H, H-4′), 4.27 (m, 1H, H-2′), 4.22 (m, 1H, H-1′), 2.71 (ddd, 1H, H-2′a, $J_{2'a,\ 3'}$=1.2 Hz, $J_{2'a,\ 1'}$=4.4 Hz, $J_{2'a,\ 2'b}$=11.2 Hz), 2.53 (m, 1H, H-2′), 2.45, 2.42, 2.40 (each s, each 3H, Ts-CH_3, Tol-CH_3), 2.28 (ddd, 1H, H-2′b, $J_{2'b,\ 3'}$=5.2 Hz, $J_{2'b,\ 1'}$=6.8 Hz, $J_{2'b,\ 2'a}$=11.2 Hz), 1.58 (s, 3H, 5-CH_3)

^{13}C NMR ($CDCl_3$, 100 MHz): δ 166.05, 166.12, 162.81, 150.60, 144.70, 144.57, 144.55, 132.86, 132.77, 129.79, 129.50, 129.46, 129.28, 127.79, 126.48, 126.25, 110.52, 85.72, 82.86, 77.21, 74.89, 66.30, 64.14, 39.73, 38.09, 21.71, 21.66, 21.55, 12.75

FAB-MS: *m/z*=677 [M+H].

2.5. Radiosynthesis of [^{18}F]NFT202 (6)

[^{18}F]Fluoride was produced with an OSCAR3 cyclotron (Oxford Instruments, Oxon, UK) using ^{18}O-enriched water and ^{18}O(p,n)^{18}F reaction. [^{18}F]Fluoride was separated with an anion exchange resin (SepPak QMA; Nihon Waters KK, Tokyo, Japan). Elution with 66 mM aqueous potassium

carbonate (0.75 ml, 5 μmol) resulted in a solution of potassium [^{18}F]fluoride.

[^{18}F]Fluoride dissolved in 66 mM aqueous potassium carbonate (0.75 ml, 5 μmol) was added to a solution of Kryptofix 222 (3.7 mg, 10 μmol; Merck Schuchardt, Hohenbrunn, Germany) in 0.25 ml of acetonitrile. The solvents were removed azeotropically with acetonitrile under a slight flow of helium at 110°C. This procedure was conducted thrice in total with 1.0 ml of dry acetonitrile. Thereafter, Compound **4** (13.5 mg, 20 μmol) in 1.0 ml of dry acetonitrile was added, after which the reaction mixture was heated to 130°C for 5 min (Scheme 2). After cooling to room temperature, 0.24 M sodium ethoxide ethanol solution (1.0 ml, 0.24 mmol) was added, and the reaction mixture was allowed to stand at room temperature for 10 min. The mixture was neutralized by the addition of 1.0 M aqueous sodium acetate (0.3 ml, 0.3 mmol). [^{18}F]NFT202 (**6**) was purified by high-performance liquid chromatography (HPLC) with a preparative column [300×30 (i.d.) mm, Develosil ODS-UG5; Nomura Chemical Co., Ltd., Tokyo, Japan]. The eluent consisted of 25% ethanol in water, and the flow was 6.0 ml/min. The radioactive fraction, eluted with a retention time corresponding to nonradioactive NFT202, synthesized as previously described (companion paper), was collected. After HPLC purification, the solvents were evaporated at 110°C and dissolved in physiological saline solution (decay-corrected radiochemical yield: 81.0±13.9%). The radiochemical purity of the [^{18}F]NFT202-injectable solution was 98.3±1.5%.

2.6. 3′-[^{18}F]3′-Fluoro-3′-deoxythymidine ([^{18}F]FLT)

[^{18}F]FLT was synthesized by a previously published method [2]. The radioactive fraction, eluted with a retention time corresponding to nonradioactive FLT (Sigma-Aldrich Japan KK, Tokyo, Japan), was collected. After HPLC purification, the decay-corrected radiochemical yield was 29.7±7.4%. The radiochemical purity of the [^{18}F]FLT-injectable solution was 95.3±4.0%.

2.7. [^{14}C]NFT202

With 2-fluoroethanol as a starting material, 2-fluoroethyltosylate was synthesized according to the method of Edgell and Parts [3]. 2-Fluoroethyltosylate (6.8 mg, 33.8 μmol), potassium carbonate (9.3 mg, 67.6 μmol) and [^{14}C]Thd (37 MBq, 16.9 μmol) were dissolved in acetone-*N*,*N*-dimethylformamide 1:1 mixed solvent (5 ml), and the mixture was heated at 50°C for 18 h under argon atmosphere. After dilution with 10 ml of diethyl ether, the mixture was loaded onto a short silica gel column (SepPak Silica; Nihon Waters KK). The radioactive product was eluted with 10 ml of chloroform:methanol (5:1). The solvent was removed by evaporation, and the desired product (35.2 MBq, 95%) was purified by silica gel thin-layer chromatography (TLC) (chloroform:methanol=5:1). After TLC purification, the radiochemical purity of [^{14}C]NFT202 was >99%, and specific activity was 2.18 GBq/mmol (according to the specific activity of [^{14}C]Thd).

2.8. Distribution

All procedures were performed in accordance with institutional guidelines (Guidelines for Animal Experiments; University of Fukui, Fukui, Japan). Seven-week-old C57BL/6 mice were purchased from Japan SLC, Inc. (Shizuoka, Japan), and held for 1 week prior to the study. Lewis lung carcinoma (LL/2) cell lines were purchased from Dai-Nippon Seiyaku Co., Ltd. (Osaka, Japan), and were maintained in the recommended culture medium obtained from the manufacturer. The cell lines were grown in a 5% CO_2-humidified atmosphere at 37°C. Tumor-bearing mice were established by subcutaneous injection of 50×10^5 (LL/2) cells to the left shoulder of 8-week-old C57BL/6 mice. The experiments on tumor-bearing mice were performed at least 10 days after inoculation, by which time the tumors had grown to about 5 mm in diameter. A saline solution of 0.1 ml containing 1.85 MBq [^{18}F]-labeled nucleosides was administered as a bolus through the tail vein. The mice were sacrificed by blood removal from the heart under ether anesthesia at predesigned time intervals of 30, 60 and 120 min. Five to six animals were used for each time interval. Urine was collected throughout the experiment, and blood samples were obtained from the syringe used in the sacrifice. Afterwards, tissue samples were removed and weighed together with the blood samples, and urine samples were counted using a 2×2-in. NaI(Tl) scintillator interfaced to a single-channel analyzer autowell gamma counter (Ohyo Koken Kogyo, Tokyo, Japan). The percent dose per organ and the percent dose per of gram tissue were calculated without body weight normalization.

2.9. TK1-dependent cell uptake

A mouse connective tissue cell line (L-M) and its thymidine-kinase-deficient mutant L-M(TK$^-$) cell line were purchased from Dai-Nippon Seiyaku Co., Ltd. and were maintained in the recommended culture media obtained from the manufacturer. The cell lines were grown in a 5% CO_2-humidified atmosphere at 37°C. The L-M(TK$^-$) cell line lacks TK activity [4]. To clarify the TK1-specific incorporation of the nucleoside, we compared the cell uptake of [^{14}C]NFT202 between the L-M and L-M(TK$^-$) cell lines.

The cells were harvested and seeded at a concentration of 2.0×10^5 into 24-well plates, and tracer uptake experiment was performed 24 h after seeding. Thymidine-free Dulbecco's modified Eagle's medium (GIBCO, Grand Island, NY, USA) was used as assay medium. Briefly, 500 μl of assay medium containing 1.3 nmol (around 74 kBq) of each tracer was added to each well, and the plate was incubated at 37°C for 60 min. After incubation, the medium was removed, and the cells were washed thrice with ice-cold phosphate-buffered saline (PBS). After washing, cell lysis was performed with 500 μl of 0.2 N NaOH. After a liquid

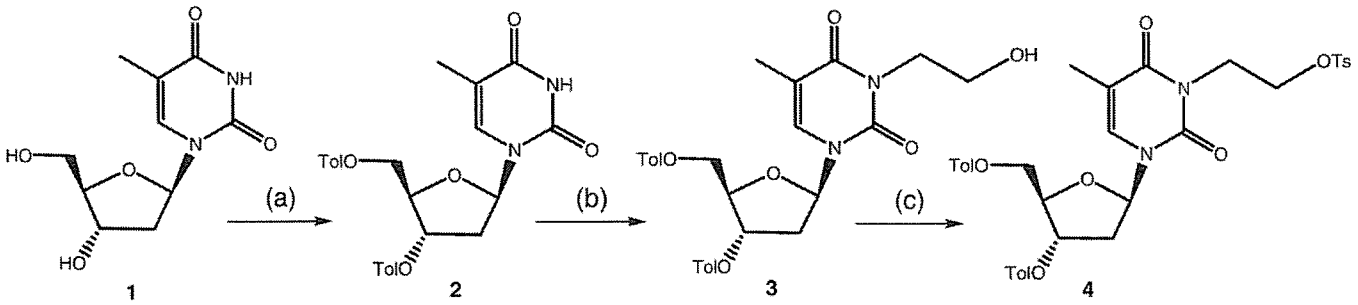

Scheme 1. Synthesis of Compound 4. Conditions: (a) *p*-toluoyl chloride (TolCl), pyridine, room temperature; (b) $BrCH_2CH_2OH$, TBAF, THF, room temperature; (c) *p*-toluenesulfonyl chloride (TsCl), pyridine, 0°C.

scintillator (ACSII; Amersham Biosciences) had been added, radioactivity in the lysate was counted using a liquid scintillation counter (LSC-5000; Aloka, Tokyo, Japan). The protein content of the lysate was then measured with the DCP protein assay reagent (Bio-Rad Japan, Tokyo, Japan). The radioactivity remaining in the wells following cell lysis was less than 5% of the total radioactivity.

2.10. Growth-dependent cell uptake

A549 human lung adenocarcinoma cells were purchased from Dai-Nippon Seiyaku Co., Ltd., and were maintained in the recommended culture medium obtained from the manufacturer. The cell lines were grown in a 5% CO_2-humidified atmosphere at 37°C.

We also compared [^{14}C]NFT202 uptake and cell cycle activity, which was expressed as the S-phase fraction. Toward this end, A549 cells were manipulated to a range of proliferation rates [from actively dividing to growth-arrested (GA)]. For plateau-phase cultures, cells were seeded at the rate of 1.0×10^4 per well in a 24-well plate with 1.0 ml of culture medium and were grown for 8 days with no change of the medium. Under these conditions, 8-day-old cultures show little or no continued growth. To analyze exponentially growing cultures, plateau-phase cultures were released by trypsin treatment and then reseeded in a fresh medium at 2×10^5 cells/well in a 24-well plate. Cell uptake was measured at 6 and 24 h after subculturing into a fresh medium. The results were compared with the uptake of cells that were not subcultured (referred to as GA cell samples).

Cell cycle distributions were determined in parallel cultures by flow cytometry. The cells from five wells were trypsinized and collected in a 15-ml culture tube (Falcon Becton Dickinson, Lincoln Park, NJ, USA). To prepare samples for DNA analysis on a flow cytometer, the cells were sedimented by centrifugation and treated with the CycleTEST PLUS DNA Reagent Kit (Becton Dickinson, San Jose, CA, USA), according to the manufacturer's instructions. The cell cycle profiles of the samples were analyzed by flow cytometry (FACS Calibur; Becton Dickinson), and the S-phase fraction was calculated by Mod-Fit LT software (Becton Dickinson).

2.11. DNA incorporation

[^{14}C]NFT202 incorporation into DNA was measured following the method described by Ayusawa et al. [5]. Briefly, after incubation with [^{14}C]NFT202, A549 cells were washed thrice with ice-cold PBS and treated with 5% trichloroacetic acid, and then the residue was washed with cold 70% ethanol. Both 5% trichloroacetic acid and 70% ethanol were collected and combined as an acid-soluble fraction, then mixed with a liquid scintillation cocktail (ACSII; Amersham Biosciences). The acid-insoluble fraction was dissolved in 0.5 ml of 0.2 N NaOH and then mixed

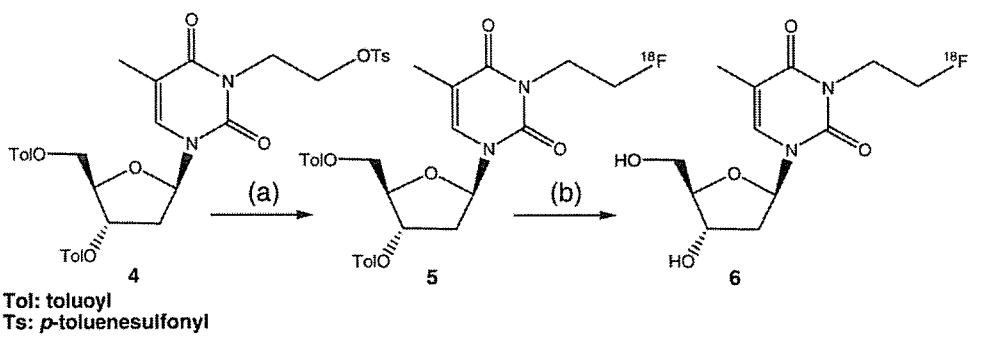

Scheme 2. Radiosynthesis of [^{18}F]NFT202 (6). Conditions: (a) $^{18}F^-$, Kryptofix 222, K_2CO_3, CH_3CN, 130°C, 5 min; (b) (i) 0.24 M sodium ethoxide (NaOEt), ethanol (EtOH), room temperature, 10 min; (ii) 1.0 M aqueous sodium acetate; (iii) semiprep HPLC (C-18, 25% EtOH).

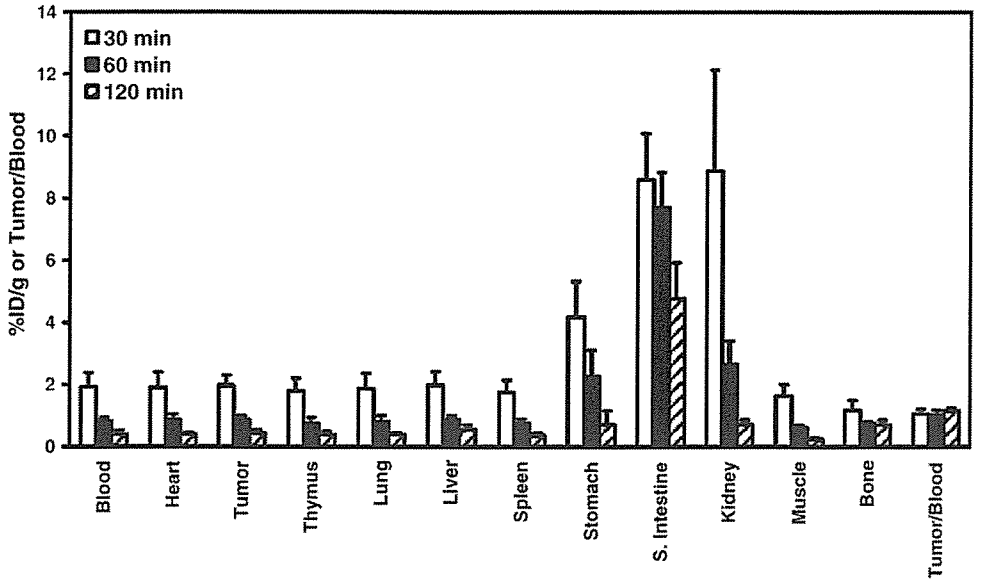

Fig. 1. Tissue distribution of radioactivity (% ID/g) or tumor/blood ratio after intravenous injection of [^{18}F]NFT202 in LL/2-bearing mice. Results are presented as mean±S.D. (n=5).

with a liquid scintillation cocktail (ACSII; Amersham Biosciences). Radioactivity was measured by a liquid scintillation counter (LSC-5100; Aloka).

3. Results

3.1. Synthesis

As outlined in Scheme 1, thymidine (**1**) was protected at the 3′,5′-di-*O*-position with toluoyl chloride in pyridine, yielding Compound **2**. The N^3 alkylation of Compound **2** was conducted in a one-pot reaction from Compound **2** by adapting a procedure described previously [6]. 2-Bromoethanol was added to a solution containing TBAF and Compound **2** in THF at room temperature, providing Compound **3** in high yield (81%). Subsequent activation of the hydroxymethyl group with tosyl chloride in pyridine gave the desired product, Compound **4**. The total yield starting from thymidine was 53%. All compounds were characterized by MS, as well as by ^{1}H and ^{13}C NMR spectroscopy. The purity of the compounds was assessed by the conspicuous absence of impurities in the ^{1}H NMR spectrum, and homogeneity was assessed by TLC.

Radiosynthesis was carried out in a two-step one-pot reaction, as outlined in Scheme 2. The fluorination reaction was conducted according to the method of Hamacher et al. [7].

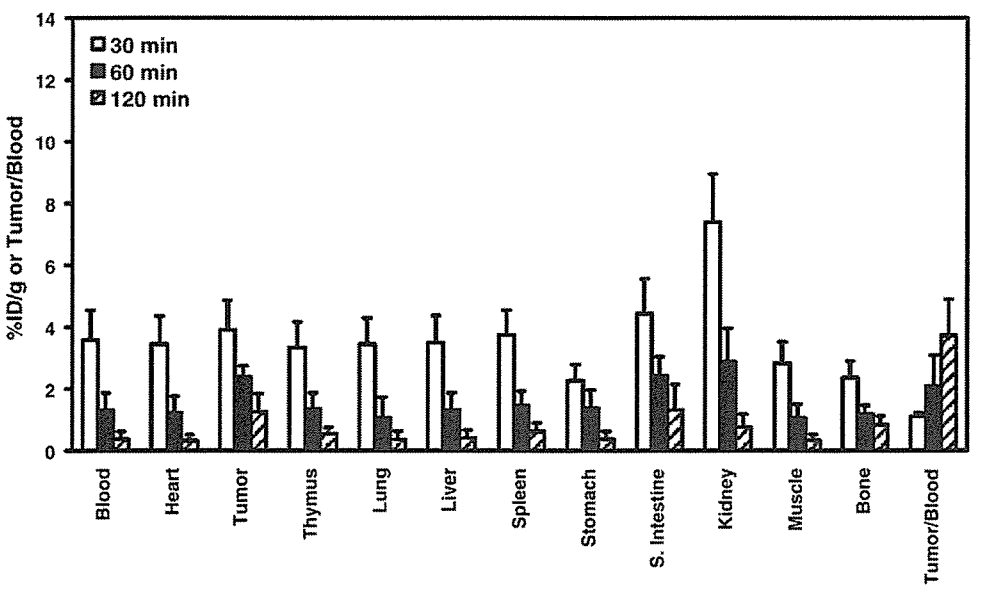

Fig. 2. Tissue distribution of radioactivity (% ID/g) or tumor/blood ratio after intravenous injection of [^{18}F]FLT into LL/2-bearing mice. Results are presented as mean±S.D. (n=5 at 30 and 60 min; n=6 at 120 min).

Thereafter, deprotection was successfully performed with 0.24 M sodium ethoxide at room temperature for 10 min. Following neutralization with 1 M sodium acetate, the crude reaction mixture was purified by HPLC, providing a [^{18}F]NFT202 solution. The decay-corrected radiochemical yield ranged from 65% to 90%. The radiochemical purity of the [^{18}F]NFT202-injectable solution ranged from 97% to 99%.

3.2. Distribution

Figs. 1 and 2 show the tissue distributions of [^{18}F]NFT202 and [^{18}F]FLT in LL/2 tumor-bearing mice, respectively. At 30 min postinjection, radioactivity concentration was lower in the blood of the former than in that of the latter, whereas at 60 min postinjection, the concentrations were the same. [^{18}F]NFT202-injected mice showed renal clearance of radioactivity [87% injected dose (ID) in urine at 120 min postinjection]. There was no significant uptake of radioactivity in the tumors of the [^{18}F]NFT202-injected mice at 120 min postinjection (tumor/blood ratio=1.14, P=.56). However, [^{18}F]FLT-injected mice showed a significantly high radioactivity uptake in the tumors at 120 min postinjection (tumor/blood ratio=3.73, P<.01). Characteristically, the [^{18}F]NFT202-injected mice showed a significantly high radioactivity uptake in the small intestines. The [^{18}F]FLT-injected mice also showed a significantly high radioactivity uptake in the small intestines. However, more radioactivity accumulated in the small intestines of the [^{18}F]NFT202-injected mice than in those of the [^{18}F]FLT-injected mice. There was no significant radioactivity uptake in the thymus or spleen of the [^{18}F]NFT202-injected mice at 120 min postinjection (thymus/blood ratio=0.95, spleen/blood ratio=0.90, P=.64). However, the [^{18}F]FLT-injected mice showed an insignificant uptake in radioactivity in the thymus and spleen at 120 min postinjection (thymus/blood ratio=1.42, P=.20; spleen/blood ratio=1.61, P=.13).

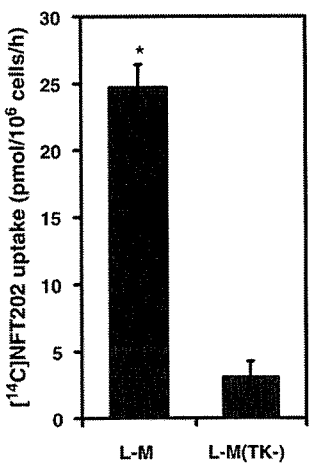

Fig. 3. Cell uptake of [^{14}C]NFT202 between the L-M parent cell and its TK mutant cell line L-M(TK$^-$). *P<.01 compared with L-M(TK$^-$) (Student's t test). Data are expressed as mean±S.D. for three experiments.

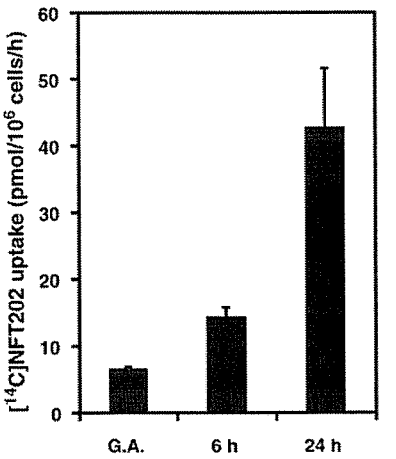

Fig. 4. Growth-dependent cell uptake of [^{14}C]NFT202. [^{14}C]NFT202 uptake was correlated with the S-phase fraction (r^2=.92). The S-phase fraction values of growth arrest, 6 h and 24 h in this experiment were 1.4, 5.1 and 24, respectively. Data are expressed as mean±S.D. for three experiments.

3.3. TK1-dependent cell uptake

The [^{14}C]NFT202 uptake in L-M cells was approximately eight times higher than that in the TK1 mutant L-M(TK$^-$) cells (Fig. 3; P<.01, Student's t test). Therefore, the cell uptake of [^{14}C]NFT202 was clearly TK1-selective.

3.4. Growth-dependent cell uptake

A549 human lung adenocarcinoma cells, with only 1.4% of the cells in the S-phase, took up little [^{14}C]NFT202. When cells were stimulated to grow by placement in a fresh medium, we observed a strong correlation between [^{14}C]NFT202 uptake and the S-phase fraction (Fig. 4; r^2=.92). Fig. 5 compares [^{14}C]FLT and [^{14}C]NFT202 uptake in A549 cells. In the high-density (slow-growth phase) and low-density (active-growth phase) conditions, [^{14}C]FLT uptake was thrice higher than [^{14}C]NFT202 uptake.

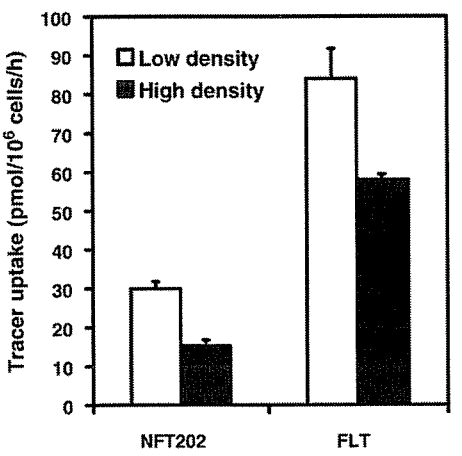

Fig. 5. [^{14}C]FLT and [^{14}C]NFT202 uptake in A549 cells. The high-density cells grew slowly and the low-density cells grew more actively. [^{14}C]FLT uptake was thrice higher than [^{14}C]NFT202 uptake. Data are expressed as mean±S.D. for three experiments.

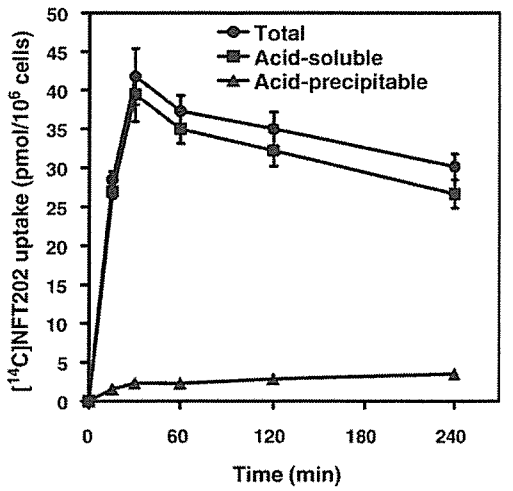

Fig. 6. Time-dependent [^{14}C]NFT202 uptake into A549 lung adenocarcinoma cells. The radioactivity of total, acid-soluble small molecules and acid-precipitable fractions (DNA) is shown. Data are expressed as mean±S.D. for three experiments.

3.5. DNA incorporation

Fig. 6 shows the time-dependent cell uptake and DNA incorporation of [^{14}C]NFT202 in A549 human lung adenocarcinoma cells. The acid-precipitable material from the DNA incorporation assay is DNA. Cellular uptake of [^{14}C]NFT202 increased until 30 min after [^{14}C]NFT202 exposure and then decreased gradually. At 240 min after [^{14}C]NFT202 exposure, the uptake was decreased to 70% of its peak uptake at 30 min. Over 90% of the radioactivity of [^{14}C]NFT202 was found in the acid-soluble fraction. DNA incorporation of [^{14}C]NFT202 was low. The low DNA incorporation was of the same level as that of FLT [8].

4. Discussion

The aim of this study was to evaluate the potential of [^{18}F]NFT202 to serve as a PET ligand for imaging cellular proliferation.

N^3-(2-fluoroethyl)-thymidine (NFT202) has been selected as a candidate cellular proliferation imaging agent because NFT202 is (a) metabolically stable against the degradation reaction of recombinant thymidine phosphorylase; (b) a potent substrate for human TK1; and (c) a high-affinity compound for nucleoside transporter. Therefore, we advanced fluorine-18 labeling of NFT202 and evaluated its suitability as a tracer for cellular proliferation imaging by PET.

Preliminarily, we synthesized three different labeling precursors possessing different 3′,5′-protecting groups (di-*O*-acetyl, di-*O*-toluoyl and di-*O*-tetrahydropyranyl) and evaluated ^{18}F fluorination yield. The best results were achieved with 3′,5′-di-*O*-toluoyl-N^3-(2-*p*-toluenesulfoxyethyl)-thymine (**4**; 81%). The labeling yields of 3′,5′-di-*O*-acetyl-N^3-(2-[^{18}F]fluoroethyl)-thymidine and 3′,5′-di-*O*-tetrahydropyranyl-N^3-(2-[^{18}F]fluoroethyl)-thymidine were 27% and 45%, respectively. Therefore, we selected Compound **4** as a labeling precursor for distribution studies.

In this study, the specific activity of the tracer was not investigated exhaustively. The typical specific activity of the [^{18}F]-labeled compound in our facility was >111 GBq/μmol [9]. In addition, our in vivo experimental system has a significant level of endogenous thymidine, which strongly reduced the in vivo uptake of thymidine analog [10]. Therefore, we evaluated the in vivo potential of [^{18}F]NFT202 by comparing it with [^{18}F]FLT.

In the present in vitro studies using L-M(TK$^-$) cells and growth-manipulated A549 lung carcinoma cells, NFT202 showed TK1-selective and growth-dependent cellular uptake. FLT also shows TK1-dependent and growth-dependent cell uptake [11]. FLT uptake correlated well (r^2=.91) with the increase in the S-phase fraction [11]. Moreover, neither NFT202 nor FLT is effectively incorporated into DNA [8]. In this sense, NFT202 and FLT are similar. However, the net uptake of NFT202 was lower than that of FLT. Moreover, the time-dependent cell uptake of NFT202 showed that NFT202 was finally washed out from the cell. NFT202 possessed the same potential for TK1 phosphorylation and enzymatic stability against TP as FLT, and it was a more suitable substrate than FLT for a nucleoside transporter. Then, what is the difference between NFT202 and FLT? Grierson et al. [1] confirmed that TK1, deoxynucleotidase (dNT) and thymidylate kinase (TMPK) are the main determinants of intracellular FLT retention, and that reversible nucleotide metabolism within the salvage pathway is a significant issue. The DNA salvage pathway involves a futile cycle for nucleoside phosphorylation and dephosphorylation mediated by TK1 and a nucleotidase dNT. This cycle poses an issue for interpreting tracer uptake values, since it provides a mechanism for the loss of established activity in cells. In addition, subsequent phosphorylation of nucleoside monophosphate by other kinases within the DNA synthesis pathway will retain the tracer because the retrograde synthesis of nucleoside from nucleoside triphosphate is thought to be negligible [1]. Therefore, the difference in cell uptake kinetics between NFT202 and FLT might be due to the dephosphorylation kinetics mediated by nucleotidase and to the affinity for other kinases within the DNA synthesis pathway: TMPK and nucleotide diphosphate kinase. These processes (reversible nucleotide metabolism within the salvage pathway) may also influence NFT202 uptake, since they provide a mechanism for the loss of established activity in cells.

The nucleoside efflux pumps also might provide a mechanism for the loss of established activity in cells. MRP8, an ATP-binding cassette transporter associated with P-glycoprotein, is known to extrude 5-fluoro-2′-deoxyuridine monophosphate from cells [12]. Grierson et al. [1] observed a small loss of FLT monophosphate (10%) to media during the efflux experiment, and they recognized that MRP8 nucleotide transporters could mediate this efflux. There is no evidence that MRP8 transports NFT202

monophosphate, but it is worth considering as a way to understand the mechanisms by which NFT202 washes out.

In several ways, our results parallel those of previous validation studies with FLT, in particular uptake/washout studies in A549 cells [1]. These results suggested that an assay for dNT activity and thymidylate kinase activity would have definitively shown which analogs were deserving of further effort.

We preliminarily analyzed the plasma metabolite of the [^{18}F]NFT202-injected mice (data not shown). Plasma radioactivity during the first 30 min was due predominantly to [^{18}F]NFT202 (80%). The intact [^{18}F]NFT202-derived radioactivity in plasma was reduced to 45% at 120 min postinjection. On the other hand, in another tumor-bearing mouse model, plasma radioactivity during the first 60 min was predominantly due to intact [^{18}F]FLT (96%) [13]. Thus, FLT seems to have an advantage in delivery due to higher blood levels. Despite this advantage, FLT shows a tumor/blood advantage only after 60 min. Therefore, tumor delivery of the tracer does not seem to be an important factor in tumor/blood ratio. Barthel et al. [14] reported that in vivo [^{18}F]FLT kinetics depends on TK1 protein expression. However, NFT202 possessed the same potential for TK1 phosphorylation as FLT. The discrepancy in the in vivo efficacy between NFT202 and FLT also may reveal the importance of reversible nucleotide metabolism within the salvage pathway, which determines intracellular nucleoside retention.

Among highly proliferating tissues, only the small intestines showed a significant uptake of [^{18}F]NFT202. However, over 70% of the radioactivity was distributed in the content, with only the remaining 30% trapped in the tissues (data not shown). This observation showed that [^{18}F]NFT202 or its metabolite was excreted through the liver into the intestine and/or was actively transported from the basal side to the apical side through the intestinal epithelial cell membrane. From another point of view, even in the most highly proliferating tissues in rodents, [^{18}F]NFT202 was not effectively trapped.

Considering these results, we concluded that [^{18}F]NFT202 is not a suitable PET ligand for imaging tumor cell proliferation. Consistent with previous validation studies [1], our results also suggested that, in order to predict in vivo performance of nucleoside derivatives, we should consider the detailed cellular and molecular biochemistry of nucleoside metabolism.

Acknowledgments

We thank Mr. Kenji Frutuka for his excellent assistance with MS analysis.

References

[1] Grierson JR, Schwartz JL, Muzi M, Jordan R, Krohn KA. Metabolism of 3′-deoxy-3′-[F-18]fluorothymidine in proliferating A549 cells: validations for positron emission tomography. Nucl Med Biol 2004; 31:829–37.

[2] Martin SJ, Eisenbarth JA, Wagner-Utermann U, Mier W, Henze M, Pritzkow H, et al. A new precursor for the radiosynthesis of [^{18}F]FLT. Nucl Med Biol 2002;29:263–73.

[3] Edgell WF, Parts L. Synthesis of alkyl and substituted alkyl fluorides from *p*-toluenesulfonic acid esters. The preparation of *p*-toluenesulfonic acid esters of lower alcohols. J Am Chem Soc 1955;77:4899–902.

[4] Kit S, Dubbes DR, Piekarski LJ, Hsu TC. Deletion of thymidine kinase activity from L cells resistant to bromodeoxyuridine. Exp Cell Res 1963;31:297–312.

[5] Ayusawa D, Shimizu K, Koyama H, Kaneda S, Takeishi K, Seno T. Cell-cycle-directed regulation of thymidylate synthase messenger RNA in human diploid fibroblasts stimulated to proliferate. J Mol Biol 1986;190:559–67.

[6] Chi DY, Kilbourn MR, Katzenellenbogen JA, Brodack JW, Welch MJ. Synthesis of no-carrier-added *N*-([^{18}F]fluoroalkyl)spiperone derivatives. Appl Radiat Isot 1986;37:1173–80.

[7] Hamacher K, Coenen HH, Stocklin G. Efficient stereospecific synthesis of no-carrier-added 2-[^{18}F]-fluoro-2-deoxy-D-glucose using aminopolyether supported nucleophilic substitution. J Nucl Med 1986;27: 235–8.

[8] Toyohara J, Waki A, Takamatsu S, Yonekura Y, Magata Y, Fujibayashi Y. Basis of FLT as a cell proliferation marker: comparative uptake studies with [^{3}H]thymidine and [^{3}H]arabinothymidine, and cell-analysis in 22 asynchronously growing tumor cell lines. Nucl Med Biol 2002;29:281–7.

[9] Mori T, Kasamatsu S, Mosdzianowski C, Welch MJ, Yonekura Y, Fujibayashi Y. Automatic synthesis of 16α-[^{18}F]fluoro-17β-estradiol ([^{18}F]FES) using a cassette-type [^{18}F]fluorodeoxyglucose synthesizer. Nucl Med Biol 2006;33:281–6.

[10] van Waarde A, Cobben DC, Suurmeijer AJ, Maas B, Vaalburg W, de Vries EF, et al. Selectivity of ^{18}F-FLT and ^{18}F-FDG for differentiating tumor from inflammation in a rodent model. J Nucl Med 2004;45: 695–700.

[11] Rasey JS, Grierson JR, Wiens LW, Kolb PD, Schwartz JL. Validation of FLT uptake as a measure of thymidine kinase-1 activity in A549 carcinoma cells. J Nucl Med 2002;43:1210–7.

[12] Guo Y, Kotova E, Chen Z-S, Lee K, Hopper-Borge E, Belinsky MG, et al. MRP8, ATP-binding cassette C11 (ABCC11), is a cyclic nucleotide efflux pump and a resistance factor for fluoropyrimidines 2′,3′-dideoxycytidine and 9′-(2′-phosphonylmethoxyethyl)adenine. J Biol Chem 2003;278:29509–14.

[13] Barthel H, Cleij MC, Collingridge DR, Hutchinson OC, Osman S, He Q, et al. 3′-Deoxy-3′-[^{18}F]fluorothymidine as a new marker for monitoring tumor response to antiproliferative therapy in vivo with positron emission tomography. Cancer Res 2003;63:3791–8.

[14] Barthel H, Perumal M, Latigo J, He Q, Brady F, Luthra SK, et al. The uptake of 3′-deoxy-3′-[^{18}F]fluorothymidine into L5178Y tumors in vivo is dependent on thymidine kinase 1 protein levels. Eur J Nucl Med Mol Imaging 2005;32:257–63.

資料(4)

Available online at www.sciencedirect.com
ScienceDirect
Nuclear Medicine and Biology 33 (2006) 743–750
NUCLEAR MEDICINE — AND — BIOLOGY
www.elsevier.com/locate/nucmedbio

Double-tracer autoradiography with Cu-ATSM/FDG and immunohistochemical interpretation in four different mouse implanted tumor models

Takeshi Tanaka[a], Takako Furukawa[b], Shigeharu Fujieda[a], Shingo Kasamatsu[b], Yoshiharu Yonekura[b], Yasuhisa Fujibayashi[b,*]

[a]*Department of Otorhinolaryngology, University of Fukui, Matsuoka, Eiheiji-cho, Yoshida-gun, Fukui 910-1193, Japan*
[b]*Biomedical Imaging Research Center, University of Fukui, Matsuoka, Eiheiji-cho, Yoshida-gun, Fukui 910-1193, Japan*

Received 11 January 2006; received in revised form 10 May 2006; accepted 15 May 2006

Abstract

Background: We studied the regional characteristics within tumor masses using PET tracers and immunohistochemical methods.
Methods: The intratumoral distribution of ^{64}Cu-diacetyl-bis(N4-methylthiosemicarbazone) ([^{64}Cu]Cu-ATSM) and [^{18}F] 2-fluoro-2-deoxyglucose ([^{18}F]FDG) in mice with tumors of four different origins (LLC1, Meth-A, B16 and colon26) was compared with the immunohistochemical staining of proliferating cells (Ki67), blood vessels (CD34 or von Willebrand factor), and apoptotic cells (terminal deoxynucleotidyltransferase-mediated dUTP nick end labeling method).
Results: With all cell lines, [^{64}Cu]Cu-ATSM and [^{18}F]FDG were distributed with different gradation in the tumor mass. The immunohistochemical study demonstrated that the high [^{64}Cu]Cu-ATSM uptake regions were hypovascular and consisted of tumor cells arrested in the cell cycle, whereas the high [^{18}F]FDG uptake regions were hypervascular and consisted of proliferating cells.
Conclusion: In our study, it was revealed that one tumor mass contained two regions with different characteristics, which could be distinguished by [^{64}Cu]Cu-ATSM and [^{18}F]FDG. Because hypoxia and cell cycle arrest are critical factors to reduce tumor sensitivity to radiation and conventional chemotherapy, regions with such characteristics should be treated intensively as one of the primary targets. [^{64}Cu]Cu-ATSM, which can delineate hypoxic and cell cycle-arrested regions in tumors, may provide valuable information for cancer treatment as well as possibly for treating such regions directly as an internal radiotherapy reagent.

Keywords: Cu-ATSM; FDG; Hypoxia; Immunohistochemistry; Cancer imaging

1. Introduction

Tumor hypoxia is associated with resistance to radiotherapy and some chemotherapy. In addition, it increases tumor aggressiveness, metastatic potential, and angiogenesis, which lead to malignant progression [1,2]. Therefore, the detection of tumor hypoxia is important to predict tumor malignancy and to determine a medical treatment plan.

Cu-diacetyl-bis(N4-methylthiosemicarbazone) (Cu-ATSM) is reduced and trapped in cells under hypoxia, but not under normoxia. When labeled with a positron-emitting radioisotope of Cu, such as ^{60}Cu, ^{61}Cu, ^{62}Cu or ^{64}Cu, it works as a PET imaging agent to detect hypoxic tumors and hypoxic regions within a tumor mass [3–5]. [^{18}F] 2-Fluoro-2-deoxyglucose ([^{18}F]FDG) is widely used as a tracer of glucose uptake by tumors. Recent studies have indicated that [^{18}F]FDG uptake is increased in hypoxic cells in culture and in hypoxic regions within tumor xenografts [6–8]. This suggests the possibility that PET with [^{18}F]FDG could provide information about hypoxia in tumor and that the intratumoral distribution of [^{18}F]FDG and [^{64}Cu]Cu-ATSM might show some similarity. However, in our previous study, in which [^{64}Cu]Cu-ATSM and [^{18}F]FDG were coinjected into rabbits with a VX2 tumor, there was a significant difference between the intratumoral distribution of [^{64}Cu]Cu-ATSM and [^{18}F]FDG: [^{64}Cu]Cu-ATSM was highly accumulated at the edge of the tumor, whereas [^{18}F]FDG was highest inside the highest [^{64}Cu]Cu-ATSM region, although it was found in all areas [9]. This indicated that the uptake patterns of [^{64}Cu]Cu-ATSM and [^{18}F]FDG into tumor cells are different.

* Corresponding author. Tel.: +81 776 61 8491; fax: +81 776 61 8170.
E-mail addresses: wplants@mac.com (T. Tanaka), yfuji@fmsrsa.fukui-med.ac.jp (Y. Fujibayashi).

0969-8051/$ – see front matter © 2006 Elsevier Inc. All rights reserved.
doi:10.1016/j.nucmedbio.2006.05.005